Neuron
Case Study

Single-Neuron Correlates of Atypical Face Processing in Autism

Ueli Rutishauser,[1,2,5,*] Oana Tudusciuc,[4] Shuo Wang,[5] Adam N. Mamelak,[1] Ian B. Ross,[6] and Ralph Adolphs[3,4,5]
[1]Department of Neurosurgery
[2]Department of Neurology
Cedars-Sinai Medical Center, Los Angeles, CA 90048, USA
[3]Division of Biology
[4]Humanities and Social Sciences
[5]Computation and Neural Systems Program
California Institute of Technology, Pasadena, CA 91125, USA
[6]Huntington Memorial Hospital, Pasadena, CA 91105, USA
*Correspondence: rutishauseru@csmc.edu
http://dx.doi.org/10.1016/j.neuron.2013.08.029

SUMMARY

People with autism spectrum disorder (ASD) show abnormal processing of faces. A range of morphometric, histological, and neuroimaging studies suggest the hypothesis that this abnormality may be linked to the amygdala. We recorded data from single neurons within the amygdalae of two rare neurosurgical patients with ASD. While basic electrophysiological response parameters were normal, there were specific and striking abnormalities in how individual facial features drove neuronal response. Compared to control patients, a population of neurons in the two ASD patients responded significantly more to the mouth, but less to the eyes. Moreover, we found a second class of face-responsive neurons for which responses to faces appeared normal. The findings confirm the amygdala's pivotal role in abnormal face processing by people with ASD at the cellular level and suggest that dysfunction may be traced to a specific subpopulation of neurons with altered selectivity for the features of faces.

INTRODUCTION

Social dysfunction is one of the core diagnostic criteria for autism spectrum disorders (ASD) and is also the most consistent finding from cognitive neuroscience studies (Chevallier et al., 2012; Gotts et al., 2012; Losh et al., 2009; Philip et al., 2012). Although there is evidence for global dysfunction at the level of the whole brain in ASD (Amaral et al., 2008; Anderson et al., 2010; Dinstein et al., 2012; Geschwind and Levitt, 2007; Piven et al., 1995), several studies emphasize abnormalities in the amygdala both morphometrically (Ecker et al., 2012) and in terms of functional connectivity (Gotts et al., 2012). Yet all functional data thus far come from studies that have used neuroimaging or electroencephalography, leaving important questions about their precise source and neuronal underpinnings. We capitalized on the comorbidity between epilepsy and ASD (Sansa et al., 2011) with the ability to record from clinically implanted depth electrodes in patients with epilepsy who are candidates for neurosurgical temporal lobectomy. This gave us the opportunity to record intracranially from the amygdala in two rare neurosurgical patients who had medically refractory epilepsy, but who also had a diagnosis of ASD, comparing their data to those obtained from eight control patients who also had medically refractory epilepsy and depth electrodes in the amygdala, but who did not have a diagnosis of ASD (see Tables S1 and S2 available online for characterization of all the patients).

Perhaps the best-studied aspect of abnormal social information processing in ASD is face processing. People with ASD show abnormal fixations onto (Kliemann et al., 2010; Klin et al., 2002; Neumann et al., 2006; Pelphrey et al., 2002; Spezio et al., 2007b) and processing of (Spezio et al., 2007a) the features of faces. A recurring pattern across studies is the failure to fixate and to extract information from the eye region of faces in ASD. Instead, at least when high functioning, people with ASD may compensate by making exaggerated use of information from the mouth region of the face (Neumann et al., 2006; Spezio et al., 2007a), a pattern also seen, albeit less prominently, in their first-degree relatives (Adolphs et al., 2008). Such compensatory strategies may also account for the variable and often subtle impairments that have been reported regarding recognition of emotions from facial expressions in ASD (Harms et al., 2010; Kennedy and Adolphs, 2012).

These behavioral findings are complemented by findings of abnormal activation of the amygdala in neuroimaging studies of ASD (Dalton et al., 2005; Kleinhans et al., 2011; Kliemann et al., 2012), an anatomical link also supported by results from genetic relatives (Dalton et al., 2007). Furthermore, neurological patients with focal bilateral amygdala lesions show intriguing parallels to the pattern of facial feature processing seen in ASD, also failing to fixate and use the eye region of the face (Adolphs et al., 2005). The link between the amygdala and fixation onto the eye region of faces (Dalton et al., 2005; Kleinhans et al., 2011; Kliemann et al., 2012) is also supported by a correlation between amygdala volume and eye fixation in studies of monkeys (Zhang et al., 2012), and by neuroimaging studies in healthy participants that have found correlations between the

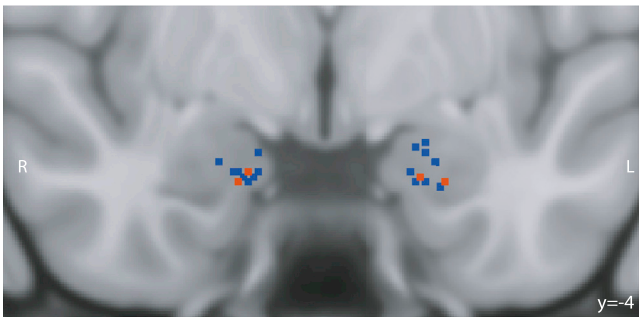

Figure 1. Recording Sites

Shown is a coronal MRI scan in MNI space showing the superposition of recording sites from the two patients with ASD (red) and controls (blue); image in radiological convention so that the left side of the brain is on the right side of the image. Recording locations were identified from the postimplantation structural MRI scans with electrodes in situ in each patient and coregistered to the MNI template brain (see Experimental Procedures). The image projects all recording locations onto the same A-P plane (y = −4) for the purpose of the illustration. Detailed anatomical information for each recording site is provided in Figure S1.

propensity to make a saccade toward the eye region and blood oxygen-level-dependent (BOLD) signal in the amygdala (Gamer and Büchel, 2009). The amygdala's role in face processing is clearly borne out by electrophysiological data: single neurons in the amygdala respond strongly to images of faces, in humans (Fried et al., 1997; Rutishauser et al., 2011) as in monkeys (Gothard et al., 2007; Kuraoka and Nakamura, 2007).

The amygdala's possible contribution to ASD is supported by a large literature showing structural and histological abnormalities (Amaral et al., 2008; Bauman and Kemper, 1985; Ecker et al., 2012; Schumann and Amaral, 2006; Schumann et al., 2004) as well as atypical activation across BOLD-fMRI studies (Gotts et al., 2012; Philip et al., 2012). Yet despite the wealth of suggestive data linking ASD, the amygdala, and abnormal social processing, data broadly consistent with long-standing hypotheses about the amygdala's contribution to social dysfunction in autism (Baron-Cohen et al., 2000), there are as yet no such studies at the neuronal level. This gap in our investigations is important to fill for several reasons. First and foremost, one would like to confirm that the prior observations translate into abnormal electrophysiological responses from neurons within the amygdala, rather than constituting a possible epiphenomenon arising from altered inputs due to more global dysfunction, or from structural abnormalities in the absence of any clear functional consequence. Moreover, such findings should also yield a deeper understanding of precisely which functional abnormalities can be attributed to the amygdala: are there nonspecific electrophysiological deviations, or is the dysfunction more specific to processing faces? Are all neurons dysfunctional, or might there be some populations that are abnormal whereas others are not? Answers at this level of analysis would help considerably in constraining the interpretations from neuroimaging studies, would allow the formulation of more precise hypotheses about the amygdala's putative role in social dysfunction in autism, and would better leverage animal models of autism that could be investigated at the cellular level.

Here we recorded from single neurons in the amygdalae of two rare neurosurgical patients with ASD. Basic electrophysiological response parameters as well as overall responsiveness to faces were comparable to responses recorded from a control patient group without ASD. However, there were specific differences in how individual facial features drove neuronal responses: neurons in the two ASD patients responded significantly more to the mouth, but less to the eyes. Additional analyses showed that the findings could not be attributed to differential fixations onto the stimuli, or to differential task difficulty, but that they did correlate with behavioral use of facial features to make emotion judgments.

RESULTS

Basic Electrophysiological Characterization and Task Performance

We isolated a total of 144 amygdala neurons from neurosurgical patients who had chronically implanted clinical-research hybrid depth electrodes in the medial temporal lobe (see Figures 1 and S1 for localization of all recording sites within the amygdala). Recordings were mostly from the basomedial and basolateral nucleus of the amygdala (see Experimental Procedures for details). We further considered only those units with firing rate $\geq$0.5 Hz (n = 91 in total, 37 from the patients with ASD). Approximately half the neurons (n = 42 in total, 19 from the patients with ASD) responded significantly to faces or parts thereof, whereas only 14% responded to a preceding "scramble" stimulus compared to baseline (Tables S3 and S4; cf. Figure 3A for stimulus design). Waveforms and interspike interval distributions looked indistinguishable between neurons recorded from the ASD patients and controls (Figure 2). To characterize basic electrophysiological signatures more objectively, we quantified the trough-to-peak time for each mean waveform of each neuron that was included in our subsequent analyses (Figure 2 and Experimental Procedures), a variable whose distribution was significantly bimodal with peaks around 0.4 and 1 ms (Hartigan's dip test, $p < 1 \times 10^{-10}$) for neurons in both subject groups, consistent with prior human recordings (Viskontas et al., 2007). The distribution of trough-to-peak times was statistically indistinguishable between the two subject groups (Kolmogorov-Smirnov test, p = 0.16). We quantified the variability of the spike times of each cell using a burst index and a modified coefficient-of-variation (CV_2) measure and found no significant differences in either measure when comparing neurons between the two subject groups (paired t tests, $p > 0.05$; see Table S5). Similarly, measures of the variability of the spiking response (see Experimental Procedures) following stimulus onset did not differ between cells recorded in ASD patients and controls (mean CV in ASD 1.02 ± 0.04 versus 0.93 ± 0.04 in controls, $p > 0.05$). Basic electrophysiological parameters characterizing spikes thus appeared to be typical in our two patients with ASD.

To investigate face processing, we used an unbiased approach in which randomly sampled pieces of emotional faces ("bubbles"; Gosselin and Schyns, 2001) were shown to participants while they pressed a button to indicate whether the

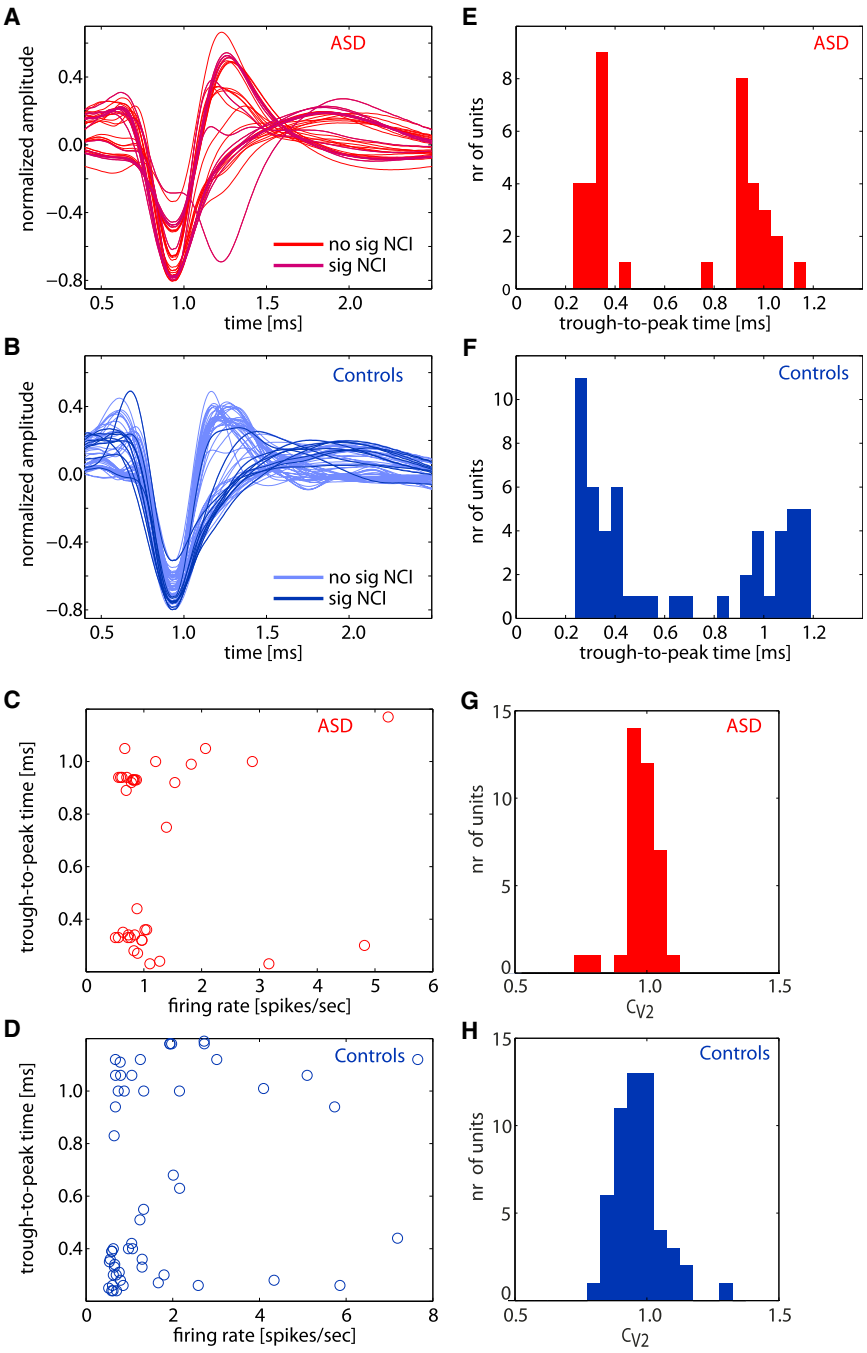

Figure 2. Electrophysiological Properties of Neurons in ASD Patients and Controls

(A and B) Mean spike waveforms (n = 37 units for ASD; n = 54 units for controls). Waveforms are shown separately for the group of cells that have significant classification images (sig NCI) and those that do not (no sig NCI, see Figure 5).

(C and D) Relationship between mean firing rate and trough-to-peak time.

(E and F) The waveforms shown in (A) and (B) quantified using their trough-to-peak times.

(G and H) Relationship between mean firing rate and coefficient of variation (CV_2). There was no significant correlation between trough-to-peak time and mean firing rate ($p > 0.05$ in both groups) and CV_2 was centered at 1 in both groups.

stimulus looked happy or fearful, a technique we have previously used to demonstrate that the amygdala is essential to process information about the eye region in faces (Adolphs et al., 2005). Complementing this data-driven approach, we also showed participants specific cutouts of the eyes and mouth, as well as the whole faces from which all these were derived (Figure 3A). The difficulty of the bubbles task was continuously controlled by adjusting the extent to which the face was revealed to achieve a target performance of 80% correct (Figure 3B shows examples). As subjects improved in performance, less of the face was revealed (as quantified by the number of bubbles) to keep the task equally difficult for all subjects. The two patients with ASD performed well on the task (Figure 3C), with accuracy as good as or exceeding that of the controls (number of bubbles for the last trial was 13.5 ± 8.5 and 20.0 ± 2.8, respectively; see Figure S2A for individual subjects). Similarly, reaction time (RT) did not differ significantly between patients with ASD and controls (relative to stimulus onset across all bubble trials, 1,357 ± 346 ms and 1,032 ± 49 ms, respectively; $p = 0.28$, two-tailed t test) although one of the ASD patients did have slower RT than any of the other participants (see Figure S2B for individual subjects). Thus, overall behavioral performance of patients with ASD did not appear impaired.

Neurons in the primate amygdala are known to respond to faces (Fried et al., 1997; Gothard et al., 2007; Kuraoka and Nakamura, 2007), and in our prior work a subpopulation of about 20% of all amygdala neurons responded more to whole faces than to any of their parts ("whole-face selective"; Rutishauser et al., 2011). Using published metrics, we here found that one-third (12/37 and 17/54, respectively) of neurons we recorded qualified as whole-face selective (WF) in the ASD and control groups. To further establish that there was no difference in the strength of face selectivity between the two subject groups, we quantified whole-face response strength relative to the response to face parts using the whole-face index (WFI, see Experimental Procedures), which quantifies the difference in firing rate between whole faces and parts (bubbles) (Rutishauser et al., 2011). The average WFI for all units recorded in the ASD patients and controls, respectively, was 19.1% ± 2.3% (n = 37) and 23.0% ± 4.5% (n = 54), respectively, which

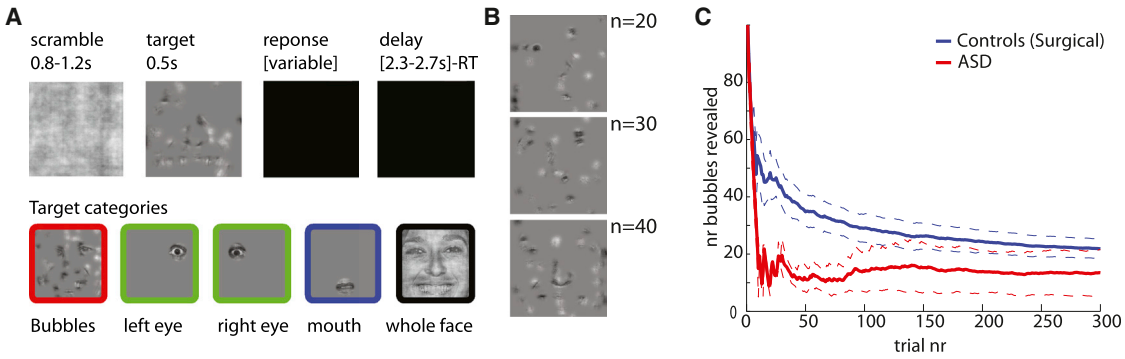

Figure 3. Task Design and Behavioral Performance

(A) Timeline of stimulus presentation and different types of stimuli used.

(B) Examples of bubbles stimuli with varying proportions of the face revealed. n is number of bubbles; same as scale in (C).

(C) Performance (number of bubbles required to maintain 80% accuracy) over time. Dotted lines are SEM.

See also Figure S2.

were not significantly different (two-tailed t test, $p = 0.45$). The average WFI for units classified as WF cells was 49.3% ± 12.1% for ASD ($n = 12$) and 60.2% ± 12.4% for controls ($n = 17$) (not significantly different, $p = 0.55$, two-tailed t test). WF cells did not differ in their basic electrophysiological properties between ASD and controls: there was no significant difference of waveform shape, burst index, or CV_2 (see Table S5). Thus, there was no significant difference in the whole-face selectivity of amygdala neurons between our two ASD subjects and controls. Together with the comparable basic electrophysiological properties we described above, this provides a common background against which to interpret the striking differences we describe next.

Abnormal Processing of the Eye Region of Faces

The "bubbles" method allows the extraction of a classification image that describes how specific (but randomly sampled) regions of a face drive a dependent measure (Adolphs et al., 2005; Gosselin and Schyns, 2001; Spezio et al., 2007a); of which we here considered two: behavioral and neural. The behavioral classification image (BCI) depicts the facial information that influences behavioral performance in the task. It is based on the correlation between the trial-by-trial appearance of any part of the face, and the RT and accuracy on that trial, calculated across all pixels and all trials (Gosselin and Schyns, 2001). The BCI showed that subjects with ASD selectively failed to make use of the eye region of faces, relying almost exclusively on the mouth (Figures 4B, 4D, S2C, and S2D), a behavioral pattern typical of people with ASD (Spezio et al., 2007a) and one that clearly distinguishes our two ASD patients from the controls (two-way ANOVA of subject group [ASD/control] by region of interest [ROI; eye/mouth] showed a significant interaction; $F(1,16) = 6.0$, $p = 0.026$; Figure 4D).

To understand what facial features were driving neuronal responses, we next computed a neuronal classification image (NCI) that depicts which features of faces were potent in modulating spike rates for a given neuron (the spike-rate-derived analog of the BCI). For each bubbles trial, we counted the number of spikes in a 1.5 s window beginning 100 ms poststimulus onset, and correlated this with the parts of the face revealed in the stimulus shown (the locations of bubbles on the face, see Experimental Procedures). This procedure results in one NCI for each neuron, summarizing the regions of the face most potent in driving its response.

We found statistically significant NCIs in approximately a third of all neurons: 43% in ASD and 19% in controls (thresholded at $p < 0.05$, corrected cluster test with $t = 2.3$, minimal cluster size 748 pixels; Table S3; see Figure S3 for single-unit examples). Strikingly, the significant NCIs in the two patients with ASD were located predominantly around the mouth region of the face, whereas those in the controls notably included the eye region (Figures 5A and S3). We quantified the mean difference in NCI Z scores within eye and mouth regions for all neurons with significant NCIs using an ROI approach (Figure 5B shows the ROIs used). The mean Z score from the NCIs of the neurons of the two patients with ASD within the mouth ROI was significantly larger than that in the controls (Figure 5C, $p < 0.0001$, two-tailed t tests throughout unless otherwise noted) and vice-versa for the eye ROIs (Figure 5D, $p < 0.0001$), an overall pattern also confirmed by a significant interaction between face region and patient group (2 × 2 ANOVA of subject group [ASD/control] by face region [eyes ROI/mouth ROI]; $F(2,68) = 14.3$, $p < 0.00001$; note this ANOVA controls for different cell numbers in different subjects using a nested random factor within the subject group factor). For the group of cells with significant NCIs, the proportion of neurons that had a higher mean Z score within the eye ROI compared to the mouth ROI was significantly smaller in ASD compared to controls (6.25% versus 60%, $p = 0.0026$, χ^2 test). In contrast, this proportion was not significantly different when considering only the neurons that did not have a significant NCI ($p = 0.26$, χ^2 test).

Our analyses utilized experimenter-defined ROIs in order to probe specific facial features. How sensitive is this analysis to the choice of ROIs we made? We conducted a complementary analysis instead using the continuous z-scored behavioral classification image obtained from the independent group of healthy nonsurgical subjects tested on the same task during eye tracking in the laboratory. This image (Figure 4C) highlights the eyes and

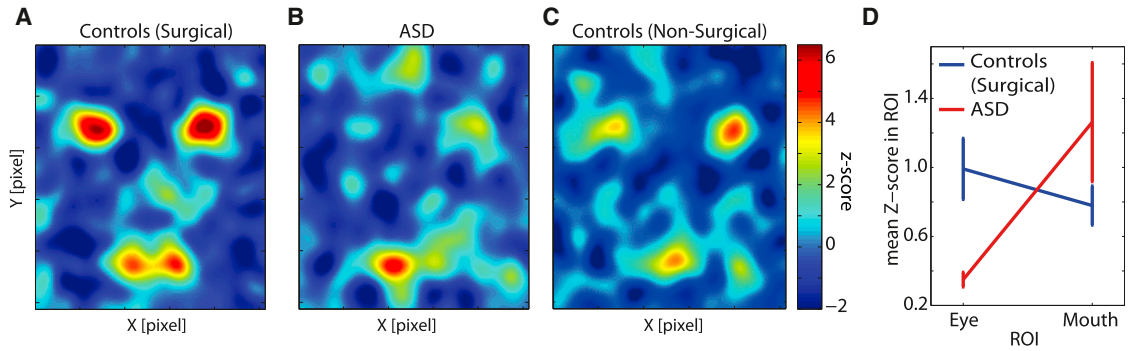

Figure 4. Average Behavioral Classification Images

(A) Surgical controls (n = 8).

(B) ASD patients (n = 2).

(C) An independent group of healthy, nonsurgical controls for comparison (n = 6). The color scale shown is valid for (A–C).

(D) Two-way ANOVA of group (ASD/epilepsy control) versus ROI (eye/mouth) showed a significant interaction ($p < 0.05$). Error bars are SEM.

See also Figure S2.

mouth, similar to our previous ROI analyses, but does so in a continuous manner directly reflecting the strength with which these regions normally drive actual behavioral emotion discrimination performance. We compared the significant NCIs obtained from each patient (Figure 5A) with this behavioral classification image (Figure 4C) by pixel-wise correlation. This analysis highlights the impaired neuronal feature selectivity in the patients with ASD: whereas the correlation was large and positive within the eye region for the controls, it was absent or negative for the patients with ASD (Figure 6; see legend for statistics and Figure S4 for individual subjects), just like their behavioral classification image was abnormal. Essentially the same pattern of results was obtained when we used as the basis for our continuous behavioral ROI the behavioral classification image derived from the surgical control patients without ASD (i.e., used Figure 4A, rather than Figure 4C).

Further Quantification of Neuronal Responses to Face Features

How representative were the neurons with significant NCIs of the population of all recorded amygdala neurons? To answer this question, we next generated continuous NCIs for all isolated neurons, regardless of whether these reached a statistically significant threshold or not. We used two approaches to quantify the NCIs of the population: first, we compared the results derived from the NCIs with those derived from independent eye and mouth cutout trials to validate the NCI approach (cf. Figure 3A for classes of stimuli used), and second, we quantified the NCIs using an ROI approach.

If an NCI obtained from the bubbles trials had its maximal *Z* score in one of the eye or mouth ROIs (Figure 5B), an enhanced response would be expected on eye or mouth cutout trials (Figure 3A), respectively. Because trials showing the cutouts were not used to compute the NCI, they constitute an independent measure of the selectivity with which neurons responded to facial features. We grouped all recorded cells according to whether their NCI had the highest *Z* score (across the entire image) in the mouth, the left eye, the right eye, or neither, and then computed the response to cutout trials for each group of neurons. We found that the response to mouth cutouts was significantly larger than to eye cutouts for neurons with high NCI *Z* scores in the mouth (n = 23, Figure S5), whereas it was significantly smaller for neurons with high NCI *Z* scores in the eyes (n = 19; difference in response to mouth minus eye cutouts −12% ± 3% versus 8% ± 3%, both significantly different from zero, $p < 0.05$). Cells that did not have a mouth- or eye-dominated NCI did not show a differential response between eye and mouth cutouts (n = 49, Figure S5). Thus, the NCIs identified a general feature sensitivity across all neurons that was replicated on the independent trials showing only mouth or eye cutouts.

Examining all neurons (n = 91), we found that the average NCI *Z* score within the mouth ROI was significantly greater in the patients with ASD compared to the controls (Figure 7A) whereas the average NCI within the eye ROI was significantly smaller (Figure 7B, $p < 0.001$ and $p < 0.00001$, respectively), a pattern again confirmed by a statistically significant interaction in a 2 × 2 ANOVA (mixed-model, see Experimental Procedures; $F(2,263) = 12.9$, $p < 0.0001$). Similarly, the proportion of all neurons that had an average NCI *Z* score that was larger in the eye ROI compared to the mouth ROI was significantly different between the two subject groups (18.9% versus 46.3%, $p = 0.0072$, χ^2 test) Thus, the impaired neuronal sensitivity to the eye region of faces in ASD that we found in Figure 5 is representative of the overall response selectivity of all recorded amygdala neurons. Interestingly, when considering the left and right eye separately we found that this difference was highly significant for the left eye (Figure 7C, $p < 0.000001$) but only marginally so for the right eye (Figure 7D, $p = 0.07$), an asymmetric pattern found in neurons from both left and right amygdalae. This finding at the neuronal level may be related to the prior finding that healthy subjects normally make more use of the left than the right eye region in this task (Gosselin et al., 2011).

Distinct Neuronal Populations Are Abnormal in ASD

There was no significant overlap between units that had significant NCIs and units that were classified as whole-face selective

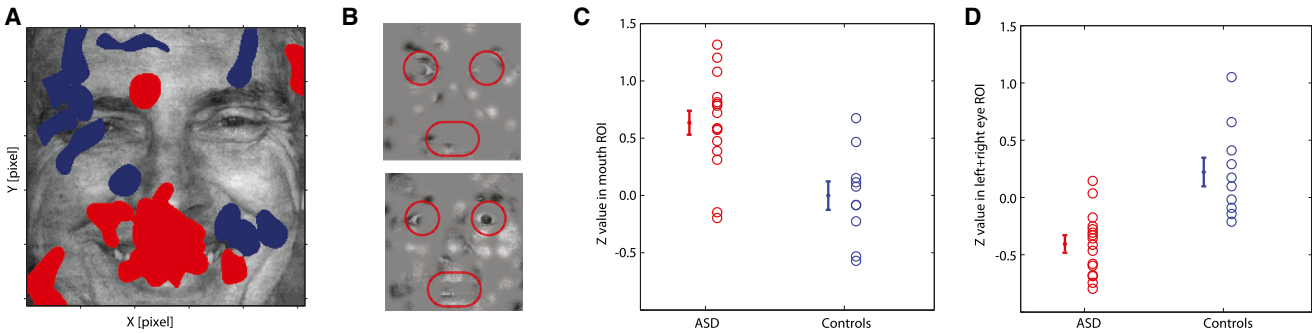

Figure 5. Neuronal Classification Images

(A) Overlay of all significant NCIs (red: ASD; blue: controls; all NCIs thresholded at cluster test $p < 0.05$ corrected; see Figure S3 for individual NCIs and their overlap).

(B) Example bubble face stimuli with the ROIs used for analysis indicated in red.

(C and D) Quantification of individual unthresholded *Z* scores for all the significant NCIs shown in (A), calculated within the mouth and eye ROIs. The overlap with the mouth ROI was significantly larger in the ASD group compared to the controls (C; $p < 0.0008$), whereas the overlap with eye ROIs was significantly smaller for the ASD group (D; $p < 0.0001$). All p values from two-tailed t tests.

from the previous analysis (2 of the 26 units with a significant NCI were also WF-selective, a proportion expected by chance alone) and there was no evidence for increased WFIs within cells that had a significant NCI (average WFI 18.0% ± 3.6% for ASD patients and 12.3% ± 3.7% for controls). We further explored the relationship between WF-selectivity and part selectivity (as evidenced by a significant NCI). We quantified each neuron's NCI by subtracting the average NCI *Z* score within the eye ROI from that in the mouth ROI. If a group of cells equally often has NCI's that focus on the eye or mouth, the average of this score should be approximately zero. On the other hand, if a group of cells is biased toward the eye or mouth, this measure will accordingly deviate from zero. We first compared all cells that were not identified as WF-selective with those that were identified as WF-selective. Note that the decision of whether a cell is WF-selective is only based on the cutout trials. The bubble trials, which are used to quantify the NCIs, remain statistically independent. Only those cells identified as not-WF selective showed a significant difference between ASD and controls, both for the entire population of cells and when restricting the analysis to only the NCI-selective cells (Figure 7E, see legend for statistics). Second, we grouped all cells according to their WFI, regardless of whether they were significant WF cells. The higher the WFI, the more a cell fires selectively for whole faces rather than any of their parts (Rutishauser et al., 2011). We found that only the cells with very low WFI differed significantly between ASD and controls. In contrast, cells with high WFIs showed no significant difference in their NCIs between ASD and controls (Figure 7F, see legend for statistics). Thus, cells with high WFI are not differentially sensitive to different facial parts in ASD, nor in controls. Taken together with our earlier findings, this suggests that not only do neurons with significant NCIs appear to be distinct from neurons with whole-face selectivity (perhaps unsurprisingly, because achieving a significant NCI requires responses to face parts), but they may in fact constitute a specific cell population with abnormal responses in ASD. The cells with significant NCIs did not differ in their basic electrophysiology between the groups (see Figure 2 for waveforms; Table S5 shows statistics). Thus, the abnormal response of NCI cells in ASD appears to reflect a true difference in facial information processing, rather than a defect in basic electrophysiological integrity of neurons within the amygdala.

To explore whether the insensitivity to eyes in ASD at the neuronal population level might be driven by the subset of cells that had a significant NCI, we further classified the cells based on their response properties. There were two groups of cells that did not have a significant NCI: those classified as WF cells, and those classified neither as NCI nor WF cells. A 2 × 2 ANOVA revealed a significant interaction only for the subset of cells that was not classified as WF ($F(2,128) = 3.5$, $p = 0.034$) but not for the cells classified as WF cells ($F(2,49) = 0.5$, $p = 0.60$). Thus, the insensitivity to eyes we found in our ASD group appears in the responses of all amygdala neurons with the exception of WF cells.

Possible Confounds

Since people with ASD may look less at eyes in faces on certain tasks (Kliemann et al., 2010; Klin et al., 2002; Neumann et al., 2006; Pelphrey et al., 2002; Spezio et al., 2007b), we wondered whether differential fixation patterns to our stimuli might explain the neuronal responses we found. This possibility seems unlikely, because by design our stimuli were of brief duration (500 ms), small (approximately 9° of visual angle), and were preceded by a central fixation cross. To verify the lack of differences in eye movements to our stimuli, we subsequently conducted high-resolution eye-tracking to the identical stimuli in the laboratory in our two epilepsy patients with ASD as well as three of the epilepsy controls from whom we had analyzed neurons. To ensure their data were representative, we also added two additional groups of subjects for comparison: six (nonsurgical) individuals with ASD (see Table S2), and six matched entirely healthy participants from the community. All made a similar and small number of fixations onto the stimuli during the 500 ms that the bubble stimuli were presented (1.5–2.5 mean fixations) and their fixation density maps did not differ (Figure 8). In particular, the average fixation density within three ROIs (both eyes, mouth, and center) showed that all subjects predominantly fixated at

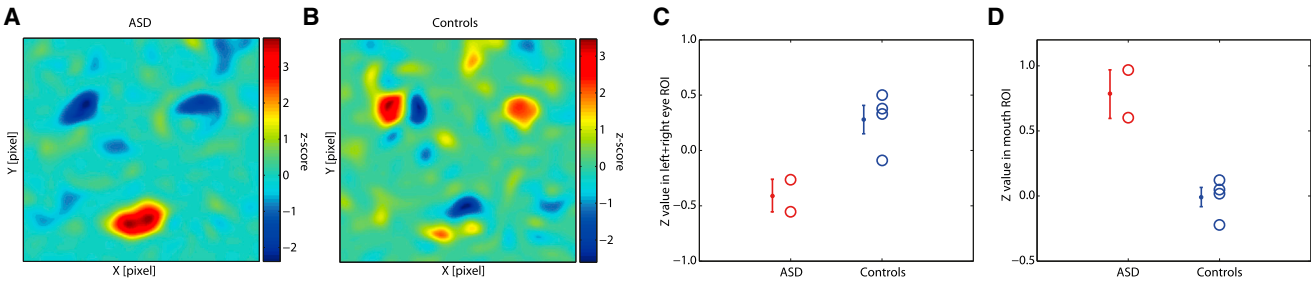

Figure 6. Correlation between Neuronal and Behavioral Classification Images

(A and B) Two-dimensional correlation between the BCI from an independent control group (Figure 4C) and the NCIs of each patient, averaged over all neurons with significant NCIs recorded in the ASD patients (A) and all recorded in the controls (B). See Figure S4 for individual correlations.

(C and D) Statistical quantification of the same data: Average values inside the mouth and eye ROIs from the two-dimensional correlations. The average Z value inside the mouth and eye ROI was significantly different between patient groups ($p = 0.031$ and $p = 0.0074$, respectively). All p values from two-tailed t tests.

the center and there was no significant dependence on subject group for fixations within any one of the three ROIs (one-way ANOVA with factor subject group, $p > 0.05$; post hoc paired t tests: ASD versus control $p = 0.34$, $p = 0.60$, $p = 0.63$ for eye, mouth, and center, respectively). Similarly, fixation density to the cutout stimuli (isolated eyes and mouth), showed no differences between groups for time spent looking at the center, eyes, or mouth ROIs (Figures S6A–S6C), even when we analyzed only the last 200ms in the trial to maximize fixation dispersion (all $p > 0.12$ from one-way ANOVAs; Figure S6 and Table S6). Finally, we repeated the above analyses for the bubbles trials also using a conditional probability approach that quantified fixation probability conditional on the region of a face being revealed on a given trial and still found no significant differences between the groups (Figure S6D; see Experimental Procedures for details).

We performed further analyses to test whether ASD and control subjects might have differed in where they allocated spatial attention. The task was designed to minimize such differences (stimuli were small and sparse and their locations were randomized to be unpredictable). Because subjects were free to move their eyes during the task, a situation in which covert and overt attention are expected to largely overlap, attentional differences would be expected to result either in overt eye gaze position or saccade latency differences, or, in the absence of eye movements, in shorter RTs to preferentially attended locations. Detailed analysis of all three of these aspects (see below) showed no significant differences between ASD and control groups.

Fixation Probability

In addition to comparing fixation probability across the different subject and control groups (see above), we also considered fixations to individually shown cutouts (left eye, right eye, and mouth) separately (Figures S6E–S6G). First, if ASD subjects make anticipatory saccades to the mouth, they would be expected to fixate there even on trials where no mouth is revealed. We found no such tendency (Figures S6E and S6F). Second, if ASD subjects pay preferential attention to the mouth, their probability of fixating the mouth should increase when regions of the mouth are revealed in a trial. We found no significant difference in the conditional fixation probability to individually shown parts (see Table S8 for statistics).

Latency of Fixations

Spatial attention might not only increase the probability of fixating but could also decrease the latency of saccades. While on most trials subjects fixated exclusively at the center of the image, they occasionally fixated elsewhere (as quantified above). We defined the saccade latency as the first point in time, relative to stimulus onset, at which the gaze position entered the eye or mouth ROI, conditional on that a saccade was made away from the center and on that this part of the face was shown in the stimulus (this analysis was carried out only for cutout trials). For the nonsurgical subjects, average saccade latencies were 199 ± 27 ms and 203 ± 30 ms, for ASD and controls, respectively (± SD, n = 6 subjects each, $p = 0.96$) and a two-way ANOVA with subject group versus ROI showed a significant main effect of ROI ($F(1,20) = 15.0$, $p < \times 10^{-4}$, a post hoc test revealed that this was due to shorter RT to eyes for both groups), but none for subject group ($F(1,20) = 1.71$) nor an interaction ($F(1,20) = 0.26$). For the surgical subjects, average saccade latencies were 204 ± 16 ms and 203 ± 30 ms, for ASD and controls, respectively, and not significantly different (two-way ANOVA showed no effect of subject group $F(1,6) = 0.37$, of ROI, $F(1,6) = 0.88$, nor interactions $F(1,6) = 0.38$). We conclude that there were no significant differences in saccade latency toward the ROIs between ASD and controls.

Reaction Times

Increased spatial attention should result in a faster behavioral response. We thus compared RT between individually shown eye and mouth cutouts as well as different categories of bubble trials (Tables S9 and S10). There was no significant difference between ASD and controls both for the surgical and nonsurgical subjects using a two-way ANOVA with the factors subject group (ASD, control) and ROI (eye, mouth) as well as post hoc pairwise tests. Another possibility is that attentional differences only emerge for stimuli through competition between different face parts, such as during some bubble trials that reveal parts of both the eye and mouth. To account for this possibility, we separated the bubbles trials into three categories (see Experimental Procedures): (1) those where mostly the eyes were shown, but little of the mouth; (2) those where mostly the mouth were shown, but little of the eyes; and (3) those where both were visible. We found no differences in RT for all three categories between

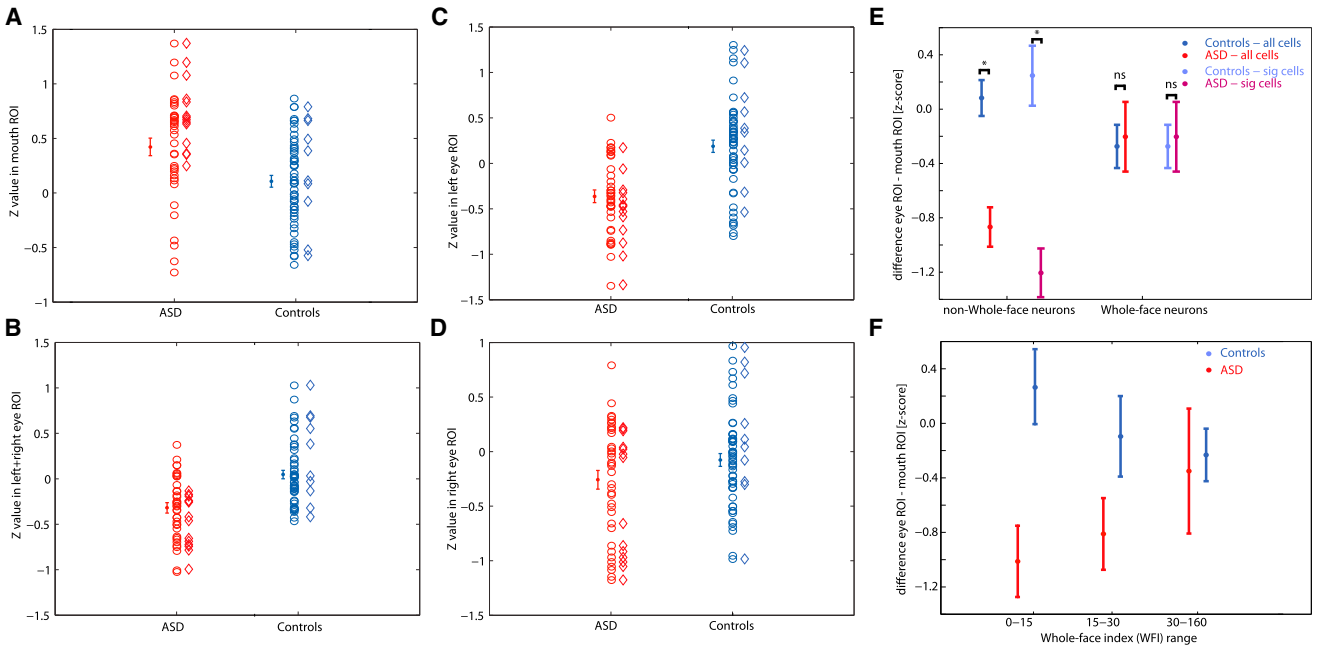

Figure 7. ROI Analyses for All Neurons Recorded

Shown are *Z* values from each neuron's NCI within the ROIs shown in Figure 5B. Cells recorded in ASD and in the controls are broken down into all (circles) and only those with statistically significant NCIs (diamonds). Error bars and statistics are based on all cells. In contrast, the data depicted in Figure 5 are based only on cells with a significant NCI.

(A) The average *Z* value inside the mouth ROI was significantly larger in ASD compared to controls ($p = 0.001$).

(B) The average *Z* value inside the eye ROI, on the other hand, was significantly smaller ($p = 2.6 \times 10^{-6}$).

(C and D) left and right eye (from the perspective of the viewer) considered separately. For both, controls had a larger *Z* value inside the eye compared to ASD, but this effect was only marginally significant for the right eye ($p = 0.07$) compared to the left eye ($p = 2.4 \times 10^{-7}$).

(E and F) Comparison of ROI analysis and whole-face responsiveness. (E) Comparison of each neuron's NCI for two groups of cells: those which were identified as WF cells (right) and those which were not identified as WF (left). For all recorded neurons (blue, red) and only those that are either identified as WF or have a significant NCI (light blue, light red), there was a significant difference in their NCIs between ASD and controls only for the cells which were not WF cells ($p = 1.3 \times 10^{-5}$ and $p = 4.4 \times 10^{-5}$, respectively, for non-WF cells; and $p = 0.81$ and $p = 0.81$ for WF cells, respectively). (F) Comparison of each neuron's NCI as a function of the WFI of each cell, regardless of whether the cell was a significant WF cell or not. Cells were grouped according to WFI alone. A significant difference was only found for cells with low WFI ($p = 0.0047$) but not for medium or large WFI values ($p = 0.10$ and $p = 0.79$, respectively).

All p values are two tailed t tests. See also Figure S5.

ASD and controls for both the surgical and nonsurgical groups (see Table S10 for statistics). We thus conclude that there were no systematic RT differences between ASD and controls.

A final possibility we considered was that the behavioral performance (button presses) of the subjects influenced their amygdala responses. This also seems unlikely because the behavioral task did not ask subjects to classify the presence or absence of the eyes or mouth, but rather to make an emotion classification (fear versus happy), and because RTs did not differ significantly between trials showing substantial eyes or mouth, nor between ASD and control groups (two-way ANOVA of subject group by ROI with RT as the dependent variable, based on cutout trials; no significant main effect of ROI, $F(1,16) = 0.5$, or subject group, $F(1,16) = 1.41$, and no significant interaction $F(1,16) = 0.81$; similar results also hold during eye tracking, see Table S9). There was no significant correlation between neuronal response and RT (only two of the 26 units with significant NCIs had a significant correlation (uncorrected), which would be expected by chance alone). Finally, the cells we identified were found to respond to a variety of features, among them the eyes and the mouth but also less common features outside those regions unrelated to the behavioral classification image (cf. Figure 5).

DISCUSSION

We compared recordings from a total of 56 neurons within the amygdala in two rare neurosurgical patients with ASD to recordings from a total of 88 neurons obtained from neurosurgical controls who did not have ASD. Basic electrophysiological response parameters of neurons did not differ between the groups, nor did the responsiveness to whole faces. Yet a subpopulation of neurons in the ASD patients—namely, those neurons that were not highly selective for whole faces, but instead responded to parts of faces—showed abnormal sensitivity to the mouth region of the face, and abnormal insensitivity to the eye region of the face. These results were obtained independently when using "bubbles" stimuli that randomly sampled regions of the face or when using specific cutouts of the eye or mouth.

The correspondence between behavioral and neuronal classification images (Figures 4A, 4B, and 5) suggests that responses

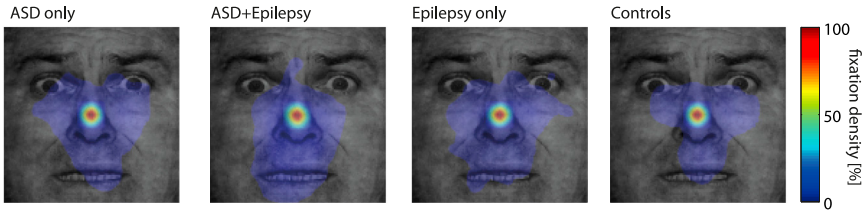

Figure 8. Eye Movements to the Stimuli
Participants saw the same stimuli and performed the same task as during our neuronal recordings while we carried out eye tracking. Data were quantified using fixation density maps that show the probability of fixating different locations during the entire 500 ms period after face onset. Shown are, from left to right, the average fixation density across subjects for ASD-only (n = 6), ASD-and Epilepsy (n = 2, same subjects as we recorded neurons from), Epilepsy-only (n = 3), and control subjects (n = 6). The scale bar (color bar) is common for all plots.
See also Figure S6.

of amygdala neurons may be related to behavioral judgments about the faces. Are the responses we recorded in the amygdala cause or consequence of behavior? We addressed several confounding possibilities above (eye movements, RT), but the question remains interesting and not fully resolved. In particular, one possibility still left open by our control analyses in this regard is that people with ASD might allocate spatial attention differentially to our stimuli, attending more to the mouth than to the eyes compared to the control participants. Although we consider this possibility unlikely, because it should be reflected in differential fixations, fixation latencies, or RTs to these facial features, it remains possible that attention could operate covertly, or perhaps at a variable level, such that these control measures would not have detected it but amygdala responses were still affected. For example, the latency of amygdala neurons in primates depends on whether value-predicting cues are presented ipsi-or contralaterally (Peck et al., 2013). Although that study confirmed that amygdala neurons are responsive to the entire visual field, it was also found that latency varied according to where visual cues were presented and firing rate correlated with RT. In contrast, we found no correlation of firing rates with RTs in the present study, but note that our task was, by construction, not a speeded RT task and subjects had ample time to respond. Future studies will be needed to provide detailed assessments of attention simultaneously with neuronal recordings; and it will also be important to make direct comparisons between complex social stimuli such as faces, and simpler conditioned visual cues.

But even if effects arising from differences in fixation and/or attention could be completely eliminated, a question remains regarding how abnormal amygdala responses could arise. The amygdala receives input about faces from cortices in the anterior temporal lobe, raising important questions regarding whether the abnormal responses we observed in patients with ASD arise at the level of the amygdala or are passed on from abnormalities already evident in temporal visual cortex. Patients with face agnosia due to damage in the temporal cortex still appear able to make normal use of the eye region of faces and render normal judgments of facial emotion (Tranel et al., 1988), whereas patients with lesions of the amygdala show deficits in both processes (Adolphs et al., 2005). These prior findings together with the amygdala's emerging role in detecting saliency (Adolphs, 2010) suggest that the abnormal feature selectivity of neurons we found in ASD may correspond to abnormal computations within the amygdala itself, a deficit that then arguably influences downstream processes including attention, learning, and motivation (Chevallier et al., 2012), perhaps in part through feedback to visual cortices (Hadj-Bouziane et al., 2012; Vuilleumier et al., 2004).

Yet the otherwise normal basic electrophysiological properties of amygdala neurons we found in ASD, together with their normal responses to whole faces (also see below), argue against any gross pathological processing within the amygdala itself. One possibility raised by a prior fMRI study is that neuronal responses might be more variable in people with ASD (Dinstein et al., 2012). We found no evidence for this in our recordings, where amygdala neurons in ASD had coefficients of variation that were equivalent for those seen in the controls (both for cells with significant NCIs as well as for whole-face cells). This finding is consistent with the data from Dinstein et al., 2012, who also found reduced signal-to-noise in BOLD responses only in the cortex, but not in subcortical structures like the amygdala. The conclusion of otherwise intact cellular function of neurons within the amygdala then raises the question of how the abnormal feature selectivity that we observed in ASD might be synthesized. One natural candidate for this is the interaction between the amygdala and the prefrontal cortex: there is evidence for abnormal connectivity of the prefrontal cortex in ASD from prior studies (Just et al., 2007), and we ourselves have found subtle deficits in functional connectivity in the brains of people with ASD that may be restricted to the anterior regions of the brain (Tyszka et al., 2013). The abnormal response selectivity in amygdala neurons we observed in ASD may thus arise from a more "top-down" effect (Neumann et al., 2006), reflecting the important role of the amygdala in integrating motivation and context—an interpretation also consistent with the long response latencies of amygdala neurons we observed.

In contrast to the abnormal responses of part-sensitive cells, whole-face selective cells in ASD subjects responded with comparable strengths as quantified by the WFI in either population group and their response was indistinguishable between different facial parts. One possible model for the generation of WF cell response properties is that these cells represent a sum over the responses of part-selective cells. This model would predict that WF cells in ASD subjects should become overly sensitive to the mouth, which we did not observe. We previously found that WF-selective cells have a highly nonlinear response to partially revealed faces (Rutishauser et al., 2011), which is also

incompatible with this model. The present findings in ASD thus add evidence to the hypothesis that WF-selective cells respond holistically to faces rather than simply summing responses to their parts.

Another key question is whether our findings are related to increased avoidance of, or decreased attraction toward, the eye region of faces. Prior findings have shown that people with ASD actively avoid the eyes in faces (Kliemann et al., 2010), and that this avoidance is correlated with BOLD response in the amygdala in neuroimaging studies (Dalton et al., 2005; Kliemann et al., 2012). However, others have found that the amygdala BOLD response in healthy individuals correlates with fixations toward the eyes (Gamer and Büchel, 2009), and one framework hypothesizes that this is decreased in ASD as part of a general reduction in social motivation and reward processing (Chevallier et al., 2012). While both active social avoidance and reduced social motivation likely contribute to ASD, future studies using concurrent eyetracking and electrophysiology could examine this complex issue further. As we noted above, in our specific task we found no evidence for differential gaze or visual attention that could explain the amygdala responses we observed. It does remain plausible, however, that the amygdala neurons we describe here in turn trigger attentional shifts at later stages in processing.

It is noteworthy that our ASD subjects were able to perform the task as well as our control subjects, showing no gross impairment. This was true both when comparing the ASD and non-ASD neurosurgical subjects (see Results), as well as when comparing nonsurgical ASD with their matched neurotypical controls (see Experimental Procedures). RTs for the neurosurgical subjects for experiments conducted in the hospital were increased by approximately 300 ms (Table S9, bottom row) relative to RTs from the laboratory outside the hospital, which is not surprising given that these experiments take place while subjects are recovering from surgery. However, this slowing affected ASD and non-ASD neurosurgical subjects equally. Unimpaired behavioral performance in emotional categorization tasks such as ours in high-functioning ASD subjects is a common finding that several previous studies demonstrated (Spezio et al., 2007a; Neumann et al., 2006; Harms et al., 2010; Ogai et al., 2003). In contrast to their normal performance, however, our ASD subjects used a distinctly abnormal strategy to solve the task, confirming earlier reports. Thus, while they performed equally well, they used different features of the face to process the task.

Brain abnormalities in ASD have been found across many structures and white matter regions, arguing for a large-scale impact on distributed neural networks and their connectivity (Amaral et al., 2008; Anderson et al., 2010; Courchesne, 1997; Geschwind and Levitt, 2007; Kennedy et al., 2006; Piven et al., 1995). Neuronal responses in ASD have been proposed to be more noisy (less consistent over time; Dinstein et al., 2012), or to have an altered balance of excitation and inhibition (Yizhar et al., 2011)—putative processing defects that could result in a global abnormality in sensory perception (Markram and Markram, 2010). The specificity of our present findings is therefore noteworthy: the abnormal feature selectivity of amygdala neurons we found in ASD contrasts with otherwise intact basic electrophysiological properties and whole-face responses. Given the case-study nature of our ASD sample together with their epilepsy and normal intellect, it is possible that our two ASD patients describe only a subset of high-functioning individuals with ASD, and it remains an important challenge to determine the extent to which the present findings will generalize to other cases. Our findings raise the possibility that particular populations of neurons within the amygdala may be differentially affected in ASD, which could inform links to synaptic and genetic levels of explanation, as well as aid the development of more specific animal models.

EXPERIMENTAL PROCEDURES

Patients

Intracranial single-unit recordings were obtained from ten neurosurgical inpatients (Table S1) with chronically implanted depth electrodes in the amygdalae for monitoring epilepsy as previously described (Rutishauser et al., 2010). Of these, only seven ultimately yielded useable single-units (the two with ASD and five without); the other three did not have ASD and provided only their behavioral performance data. Electrodes were placed using orthogonal (to the midline) trajectories and used to localize seizures for possible surgical treatment of epilepsy. We included only participants who had normal or corrected-to-normal vision, intact ability to discriminate faces on the Benton Facial Discrimination Task, and who were fully able to understand the task. Each patient performed one session of the task consisting of multiple blocks of 120 trials each (see below). While some patients performed several sessions on consecutive days, we specifically only include the first session of each patient to allow a fair comparison to the autism subjects (who only performed the task once). All included sessions are the first sessions and patients had never performed the task or anything similar before. All participants provided written informed consent according to protocols approved by the Institutional review boards of the Huntington Memorial Hospital, Cedars-Sinai Medical Center, and the California Institute of Technology.

Autism Diagnosis

The two patients with ASD had a clinical diagnosis according to DSM-IV-TR criteria and met algorithm criteria for an ASD on the Autism Diagnostic Observation Schedule. Scores on the Autism Quotient and Social Responsiveness scale, where available, further confirmed a diagnosis of ASD. All ASD diagnoses were corroborated by at least two independent clinicians blind to the identity of the participants or the hypotheses of the study. While not diagnostic, the behavioral performances of the two patients with epilepsy and ASD on our experimental task were also consistent with the behavioral performance of a different group of subjects with ASD that we had reported previously (Spezio et al., 2007a) as well as a new control group of six ASD control subjects who we tested in the present paper (see Table S2).

Electrophysiology

We recorded bilaterally from implanted depth electrodes in the amygdala. Target locations were verified using postimplantation structural MRIs (see below). At each site, we recorded from eight 40 μm microwires inserted into a clinical electrode as described previously (Rutishauser et al., 2010). Only data acquired from recording contacts within the amygdala are reported here. Electrodes were positioned such that their tips were located in the upper third to center of the deep amygdala, ~7 mm from the uncus. Microwires projected medially out at the end of the depth electrode and electrodes were thus likely sampling neurons in the midmedial part of the amygdala (basomedial nucleus or deepest part of the basolateral nucleus; Oya et al., 2009). Bipolar recordings, using one of the eight microwires as reference, were sampled at 32 kHz and stored continuously for off-line analysis with a 64-channel Neuralynx system (Digital Cheetah; Neuralynx). The raw signal was filtered and spikes were sorted using a semiautomated template-matching algorithm as described previously (Rutishauser et al., 2006). Channels with interictal epileptic spikes in the LFP were excluded. For wires which had several clusters

of spikes (47 wires had at least one unit, 25 of which had at least two), we additionally quantified the goodness of separation by applying the projection test (Rutishauser et al., 2006) for each possible pair of neurons. The projection test measures the number of SDs by which the two clusters are separated after normalizing the data, so that each cluster is normally distributed with a SD of 1. The average distance between all possible pairs (n = 170) was 12.6 ± 2.8 SD. The average SNR of the mean waveforms relative to the background noise was 1.9 ± 0.1 and the average percentage of interspike intervals that were less than 3ms (a measure of sorting quality) was 0.31 ± 0.03. All above sorting results are only for units considered for the analysis (baseline of 0.5 Hz or higher).

Stimuli and Task

Patients were asked to judge whether faces (or parts thereof) shown for 500 ms looked happy or fearful (two-alternative forced choice). Stimuli were presented in blocks of 120 trials. Stimuli consisted of bubbled faces (60% of all trials), cutouts of the eye region (left and right, 10% each), mouth region (10% of all trials), or whole (full) faces (10% of all trials) and were shown fully randomly interleaved at the center of the screen of a laptop computer situated at the patient's bedside. All stimuli were derived from the whole face stimuli, which were happy and fearful faces from the Ekman and Friesen stimulus set we used in the same task previously (Spezio et al., 2007a). Mouth and eye cutout stimuli were all the same size. Each trial consisted of a sequence of images shown in the following order: (1) scrambled face, (2) face stimulus, and (3) blank screen (cf. Figure 3A). Scrambled faces were created from the original faces by randomly re-ordering their phase spectrum. They thus had the same amplitude spectrum and average luminance. Scrambled faces were shown for 0.8–1.2 s (randomized). Immediately afterward, the target stimulus was shown for 0.5 s (fixed time), which was then replaced by a blank screen. Subjects were instructed to make their decision as soon as possible. Regardless of RT, the next trial started after an interval of 2.3–2.7 s after stimulus onset. If the subject did not respond by that time, a timeout was indicated by a beep (2.2% of all trials were timeouts and were excluded from analysis; there was no difference in timeouts between ASD patients and controls). Patients responded by pressing marked buttons on a keyboard (happy or fearful). Distance to the screen was 50 cm, resulting in a screen size of 30° × 23° of visual angle and a stimulus size of approximately 9° × 9° of visual angle. Patients completed five to seven blocks during which we collected electrophysiological data continuously (on average, 6.5 blocks for the patients with epilepsy and ASD and 5.6 for epilepsy patients without ASD, resulting in 696 ± 76 trials on average). After each block, the achieved performance was displayed on a screen to participants as an incentive.

Derivation of Behavioral and Neuronal Classification Images

BCIs were derived as described previously (Gosselin and Schyns, 2001). Briefly, the BCIs were calculated for each session based on accuracy and RT. Only bubble trials were used. Each pixel C(x,y) of the CI is the correlation of the noise mask at that pixel with whether the trial was correct/incorrect or the RT (Equation 1). Pixels with high positive correlation indicate that revealing this pixel increases task performance. The raw CI C(x,y) is then rescaled (Z scored) such that it has a Student's t distribution with N-2 degrees of freedom (Equation 2).

$$C(x,y) = \sum_{i=1}^{N} \frac{\left[X_i(x,y) - \overline{X}(x,y)\right]\left(Y_i - \overline{Y}\right)}{\sqrt{\sum_{j=1}^{N}\left[X_j(x,y) - \overline{X}(x,y)\right]^2}\sqrt{\sum_{j=1}^{N}\left(Y_j - \overline{Y}\right)^2}} \quad \text{(Equation 1)}$$

$$Z(x,y) = \sqrt{N}C(x,y) \quad \text{(Equation 2)}$$

N is the number of trials, $X_i(x,y)$ is the smoothened noise mask for trial i, Y_i the response accuracy or the RT for trial i and $\overline{X}(x,y)$ and $\overline{Y}$ is the mean over all trials. The noise masks $X_i(x,y)$ are the result of a convolution of bubble locations (where each center of a bubble is marked with a 1, the rest 0) with a 2D Gaussian kernel with width $\sigma = 10$ pixels and a kernel size of 6 σ (exactly as shown to subjects, no further smoothing is applied). Before convolution, images were zero-padded to avoid edge effects. For each session, we calculated two CIs: one based on accuracy and one based on RT. These were then averaged as $Z(x,y) = [Z_{RT}(x,y) + Z_{accuracy}(x,y)]/\sqrt{2}$ to obtain the BCI for each session. BCIs across patients were averaged using the same equation, resulting in spatial representations of where on the face image there was a significant association between that part of the face shown and accurate emotion classification (Figures 4A–4C). As a comparison, we also computed the BCIs only considering accuracy (not considering RT) and found very similar BCIs (not shown).

Neuronal classification images (NCI) were computed as shown in Equations 1 and 2; however, the response Y_i and its average $\overline{Y}$ was equivalent to spike counts in this case. Otherwise, the calculation is equivalent. Spikes were counted for each correct bubble trial i in a time window of 1.5 s length starting at 100 ms after stimulus onset. Incorrect trials are not used to construct the NCI.

An NCI was calculated for every cell with a sufficient number of spikes. The NCI has the same dimension as the image (256 × 256 pixels), but due to the structure of the noise mask used to construct the bubbles trials it is a smooth random Gaussian field in 2D. Nearby pixels are thus correlated and appropriate statistical tests need to take this into account. We used the well-established Cluster test (Chauvin et al., 2005) with t = 2.3 that has been developed for this purpose. The test enforces a minimal significance value and a minimal cluster size for an area in the NCI to be significant and multiple-comparison corrected. Note that the desired significance and the minimal cluster size are anticorrelated, i.e., if setting a low significance the minimal size of clusters considered significant increases. Our value of t = 2.3 corresponds to a minimal cluster size of 748 pixels. The NCI for a cell was considered significant if there was at least one cluster satisfying the cluster test. For plotting purposes only, thresholded CIs are shown in some figures that only reveal the proportion determined to be significant by the cluster test (specifically: Figure 5A and Figure S3). For analysis purposes, however, the raw and continuous NCI was always used. No analysis was based on thresholded behavioral or neuronal CIs, although some analyses are based on only those neurons whose NCI had regions that surpassed a statistical threshold for significance.

Data Analysis: Spikes

Only single units with an average firing rate of at least 0.5 Hz (entire task) were considered. Only correct trials were considered and all raster plots only show correct trials. In addition, the first ten trials of the first block were discarded. Trials were aligned to stimulus onset, except when comparing the baseline to the scramble-response for which trials were aligned to scramble onset (which precedes the stimulus onset). Statistical comparisons between the firing rates in response to different stimuli were made based on the total number of spikes produced by each unit in a 1 s interval starting at 250 ms after stimulus onset. Pairwise comparisons were made using a two-tailed t test at $p < 0.05$ and Bonferroni-corrected for multiple comparisons where necessary. Average firing rates (PSTH) were computed by counting spikes across all trials in consecutive 250 ms bins. To convert the PSTH to an instantaneous firing rate, a Gaussian kernel with sigma 300 ms was used (for plotting purposes only, all statistics are based on the raw counts).

Statistical Tests

Two-way ANOVAs to quantify the difference in NCIs between the ASD and control groups were performed using a mixed-model ANOVA with cell number as a random factor nested into the fixed factor subject group. ROI was a fixed factor. Cell number was a random factor because it is a priori unknown how many significant cells will be discovered in each recording session. The two-way ANOVAs to quantify the behavior (BCI and RT) had only fixed factors (subject group and ROI).

All data analysis was performed using custom written routines in MATLAB. All errors are ± SEM unless specified otherwise. All p values are from two-tailed t tests unless specified otherwise.

SUPPLEMENTAL INFORMATION

Supplemental Information includes Supplemental Experimental Procedures, six figures, and ten tables and can be found with this article online at http://dx.doi.org/10.1016/j.neuron.2013.08.029.

ACKNOWLEDGMENTS

We thank all patients and their families for their help in conducting the studies; Lynn Paul, Daniel Kennedy, and Christina Corsello for performing ADOS; Christopher Heller for neurosurgical implantation in some of our subjects; Linda Philpott for neuropsychological assessment; and William Sutherling and the staff of the Huntington Memorial Hospital for their support with the studies. We also thank Erin Schuman for advice and providing some of the electrophysiology equipment, and Frederic Gosselin, Michael Spezio, Julien Dubois, and Jeffrey Wertheimer for discussion. This research was made possible by funding from the Simons Foundation (to R.A.), the Gordon and Betty Moore Foundation (to R.A.), the Max Planck Society (to U.R.), the Cedars-Sinai Medical Center (to U.R. and A.M.), a fellowship from Autism Speaks (to O.T.), and a Conte Center from the National Institute of Mental Health (to R.A.).

Accepted: August 20, 2013
Published: November 20, 2013

REFERENCES

Adolphs, R. (2010). What does the amygdala contribute to social cognition? Ann. N Y Acad. Sci. *1191*, 42–61.

Adolphs, R., Gosselin, F., Buchanan, T.W., Tranel, D., Schyns, P., and Damasio, A.R. (2005). A mechanism for impaired fear recognition after amygdala damage. Nature *433*, 68–72.

Adolphs, R., Spezio, M.L., Parlier, M., and Piven, J. (2008). Distinct face-processing strategies in parents of autistic children. Curr. Biol. *18*, 1090–1093.

Amaral, D.G., Schumann, C.M., and Nordahl, C.W. (2008). Neuroanatomy of autism. Trends Neurosci. *31*, 137–145.

Anderson, J.S., Druzgal, T.J., Froehlich, A., DuBray, M.B., Lange, N., Alexander, A.L., Abildskov, T., Nielsen, J.A., Cariello, A.N., Cooperrider, J.R., et al. (2010). Decreased interhemispheric functional connectivity in autism. Cereb. Cortex. http://dx.doi.org/10.1093/cercor/bhq190.

Baron-Cohen, S., Ring, H.A., Bullmore, E.T., Wheelwright, S., Ashwin, C., and Williams, S.C. (2000). The amygdala theory of autism. Neurosci. Biobehav. Rev. *24*, 355–364.

Bauman, M., and Kemper, T.L. (1985). Histoanatomic observations of the brain in early infantile autism. Neurology *35*, 866–874.

Chauvin, A., Worsley, K.J., Schyns, P.G., Arguin, M., and Gosselin, F. (2005). Accurate statistical tests for smooth classification images. J. Vis. *5*, 659–667.

Chevallier, C., Kohls, G., Troiani, V., Brodkin, E.S., and Schultz, R.T. (2012). The social motivation theory of autism. Trends Cogn. Sci. *16*, 231–239.

Courchesne, E. (1997). Brainstem, cerebellar and limbic neuroanatomical abnormalities in autism. Curr. Opin. Neurobiol. *7*, 269–278.

Dalton, K.M., Nacewicz, B.M., Johnstone, T., Schaefer, H.S., Gernsbacher, M.A., Goldsmith, H.H., Alexander, A.L., and Davidson, R.J. (2005). Gaze fixation and the neural circuitry of face processing in autism. Nat. Neurosci. *8*, 519–526.

Dalton, K.M., Nacewicz, B.M., Alexander, A.L., and Davidson, R.J. (2007). Gaze-fixation, brain activation, and amygdala volume in unaffected siblings of individuals with autism. Biol. Psychiatry *61*, 512–520.

Dinstein, I., Heeger, D.J., Lorenzi, L., Minshew, N.J., Malach, R., and Behrmann, M. (2012). Unreliable evoked responses in autism. Neuron *75*, 981–991.

Ecker, C., Suckling, J., Deoni, S.C., Lombardo, M.V., Bullmore, E.T., Baron-Cohen, S., Catani, M., Jezzard, P., Barnes, A., Bailey, A.J., et al.; MRC AIMS Consortium. (2012). Brain anatomy and its relationship to behavior in adults with autism spectrum disorder: a multicenter magnetic resonance imaging study. Arch. Gen. Psychiatry *69*, 195–209.

Fried, I., MacDonald, K.A., and Wilson, C.L. (1997). Single neuron activity in human hippocampus and amygdala during recognition of faces and objects. Neuron *18*, 753–765.

Gamer, M., and Büchel, C. (2009). Amygdala activation predicts gaze toward fearful eyes. J. Neurosci. *29*, 9123–9126.

Geschwind, D.H., and Levitt, P. (2007). Autism spectrum disorders: developmental disconnection syndromes. Curr. Opin. Neurobiol. *17*, 103–111.

Gosselin, F., and Schyns, P.G. (2001). Bubbles: a technique to reveal the use of information in recognition tasks. Vision Res. *41*, 2261–2271.

Gosselin, F., Spezio, M.L., Tranel, D., and Adolphs, R. (2011). Asymmetrical use of eye information from faces following unilateral amygdala damage. Soc. Cogn. Affect. Neurosci. *6*, 330–337.

Gothard, K.M., Battaglia, F.P., Erickson, C.A., Spitler, K.M., and Amaral, D.G. (2007). Neural responses to facial expression and face identity in the monkey amygdala. J. Neurophysiol. *97*, 1671–1683.

Gotts, S.J., Simmons, W.K., Milbury, L.A., Wallace, G.L., Cox, R.W., and Martin, A. (2012). Fractionation of social brain circuits in autism spectrum disorders. Brain *135*, 2711–2725.

Hadj-Bouziane, F., Liu, N., Bell, A.H., Gothard, K.M., Luh, W.-M., Tootell, R.B.H., Murray, E.A., and Ungerleider, L.G. (2012). Amygdala lesions disrupt modulation of functional MRI activity evoked by facial expression in the monkey inferior temporal cortex. Proc. Natl. Acad. Sci. USA.

Harms, M.B., Martin, A., and Wallace, G.L. (2010). Facial emotion recognition in autism spectrum disorders: a review of behavioral and neuroimaging studies. Neuropsychol. Rev. *20*, 290–322.

Just, M.A., Cherkassky, V.L., Keller, T.A., Kana, R.K., and Minshew, N.J. (2007). Functional and anatomical cortical underconnectivity in autism: evidence from an FMRI study of an executive function task and corpus callosum morphometry. Cereb. Cortex *17*, 951–961.

Kennedy, D.P., and Adolphs, R. (2012). Perception of emotions from facial expressions in high-functioning adults with autism. Neuropsychologia *50*, 3313–3319.

Kennedy, D.P., Redcay, E., and Courchesne, E. (2006). Failing to deactivate: resting functional abnormalities in autism. Proc. Natl. Acad. Sci. USA *103*, 8275–8280.

Kleinhans, N.M., Richards, T., Johnson, L.C., Weaver, K.E., Greenson, J., Dawson, G., and Aylward, E. (2011). fMRI evidence of neural abnormalities in the subcortical face processing system in ASD. Neuroimage *54*, 697–704.

Kliemann, D., Dziobek, I., Hatri, A., Steimke, R., and Heekeren, H.R. (2010). Atypical reflexive gaze patterns on emotional faces in autism spectrum disorders. J. Neurosci. *30*, 12281–12287.

Kliemann, D., Dziobek, I., Hatri, A., Baudewig, J., and Heekeren, H.R. (2012). The role of the amygdala in atypical gaze on emotional faces in autism spectrum disorders. J. Neurosci. *32*, 9469–9476.

Klin, A., Jones, W., Schultz, R., Volkmar, F., and Cohen, D. (2002). Visual fixation patterns during viewing of naturalistic social situations as predictors of social competence in individuals with autism. Arch. Gen. Psychiatry *59*, 809–816.

Kuraoka, K., and Nakamura, K. (2007). Responses of single neurons in monkey amygdala to facial and vocal emotions. J. Neurophysiol. *97*, 1379–1387.

Losh, M., Adolphs, R., Poe, M.D., Couture, S., Penn, D., Baranek, G.T., and Piven, J. (2009). Neuropsychological profile of autism and the broad autism phenotype. Arch. Gen. Psychiatry *66*, 518–526.

Markram, K., and Markram, H. (2010). The intense world theory - a unifying theory of the neurobiology of autism. Frontiers in Human Neuroscience *4*, article 224.

Neumann, D., Spezio, M.L., Piven, J., and Adolphs, R. (2006). Looking you in the mouth: abnormal gaze in autism resulting from impaired top-down modulation of visual attention. Soc. Cogn. Affect. Neurosci. *1*, 194–202.

Ogai, M., Matsumoto, H., Suzuki, K., Ozawa, F., Fukuda, R., Uchiyama, I., Suckling, J., Isoda, H., Mori, N., and Takei, N. (2003). fMRI study of recognition of facial expressions in high-functioning autistic patients. Neuroreport *14*, 559–563.

Oya, H., Kawasaki, H., Dahdaleh, N.S., Wemmie, J.A., and Howard, M.A., 3rd. (2009). Stereotactic atlas-based depth electrode localization in the human amygdala. Stereotact. Funct. Neurosurg. *87*, 219–228.

Peck, C.J., Lau, B., and Salzman, C.D. (2013). The primate amygdala combines information about space and value. Nat. Neurosci. *16*, 340–348.

Pelphrey, K.A., Sasson, N.J., Reznick, J.S., Paul, G., Goldman, B.D., and Piven, J. (2002). Visual scanning of faces in autism. J. Autism Dev. Disord. *32*, 249–261.

Philip, R.C.M., Dauvermann, M.R., Whalley, H.C., Baynham, K., Lawrie, S.M., and Stanfield, A.C. (2012). A systematic review and meta-analysis of the fMRI investigation of autism spectrum disorders. Neurosci. Biobehav. Rev. *36*, 901–942.

Piven, J., Arndt, S., Bailey, J., Havercamp, S., Andreasen, N.C., and Palmer, P. (1995). An MRI study of brain size in autism. Am. J. Psychiatry *152*, 1145–1149.

Rutishauser, U., Schuman, E.M., and Mamelak, A.N. (2006). Online detection and sorting of extracellularly recorded action potentials in human medial temporal lobe recordings, in vivo. J. Neurosci. Methods *154*, 204–224.

Rutishauser, U., Ross, I.B., Mamelak, A.N., and Schuman, E.M. (2010). Human memory strength is predicted by theta-frequency phase-locking of single neurons. Nature *464*, 903–907.

Rutishauser, U., Tudusciuc, O., Neumann, D., Mamelak, A.N., Heller, A.C., Ross, I.B., Philpott, L., Sutherling, W.W., and Adolphs, R. (2011). Single-unit responses selective for whole faces in the human amygdala. Curr. Biol. *21*, 1654–1660.

Sansa, G., Carlson, C., Doyle, W., Weiner, H.L., Bluvstein, J., Barr, W., and Devinsky, O. (2011). Medically refractory epilepsy in autism. Epilepsia *52*, 1071–1075.

Schumann, C.M., and Amaral, D.G. (2006). Stereological analysis of amygdala neuron number in autism. J. Neurosci. *26*, 7674–7679.

Schumann, C.M., Hamstra, J., Goodlin-Jones, B.L., Lotspeich, L.J., Kwon, H., Buonocore, M.H., Lammers, C.R., Reiss, A.L., and Amaral, D.G. (2004). The amygdala is enlarged in children but not adolescents with autism; the hippocampus is enlarged at all ages. J. Neurosci. *24*, 6392–6401.

Spezio, M.L., Adolphs, R., Hurley, R.S., and Piven, J. (2007a). Abnormal use of facial information in high-functioning autism. J. Autism Dev. Disord. *37*, 929–939.

Spezio, M.L., Adolphs, R., Hurley, R.S., and Piven, J. (2007b). Analysis of face gaze in autism using "Bubbles". Neuropsychologia *45*, 144–151.

Tranel, D., Damasio, A.R., and Damasio, H. (1988). Intact recognition of facial expression, gender, and age in patients with impaired recognition of face identity. Neurology *38*, 690–696.

Tyszka, J.M., Kennedy, D.P., Paul, L.K., and Adolphs, R. (2013). Largely intact patterns of resting-state functional connectivity in high-functioning autism. Cereb. Cortex. Published online February 20, 2013. http://dx.doi.org/10.1093/cercor/bht040.

Viskontas, I.V., Ekstrom, A.D., Wilson, C.L., and Fried, I. (2007). Characterizing interneuron and pyramidal cells in the human medial temporal lobe in vivo using extracellular recordings. Hippocampus *17*, 49–57.

Vuilleumier, P., Richardson, M.P., Armony, J.L., Driver, J., and Dolan, R.J. (2004). Distant influences of amygdala lesion on visual cortical activation during emotional face processing. Nat. Neurosci. *7*, 1271–1278.

Yizhar, O., Fenno, L.E., Prigge, M., Schneider, F., Davidson, T.J., O'Shea, D.J., Sohal, V.S., Goshen, I., Finkelstein, J., Paz, J.T., et al. (2011). Neocortical excitation/inhibition balance in information processing and social dysfunction. Nature *477*, 171–178.

Zhang, B., Noble, P.L., Winslow, J.T., Pine, D.S., and Nelson, E.E. (2012). Amygdala volume predicts patterns of eye fixation in rhesus monkeys. Behav. Brain Res. *229*, 433–437.

Neuron, Volume *80*

Supplemental Information

Single-Neuron Correlates of Atypical Face Processing in Autism

Ueli Rutishauser, Oana Tudusciuc, Shuo Wang, Adam N. Mamelak, Ian B. Ross, and Ralph Adolphs

Supplementary Information

Inventory of supplementary information

The supplement for this paper consists of the following information:

Supplementary Experimental Procedures

10 supplementary tables

Supplementary references

Supplementary figures and their relationship to main paper figures:

Figure S1, related to Figure 1.

Figure S2, related to Figure 4.

Figure S3, related to Figure 5.

Figure S4, related to Figure 6.

Figure S5, related to Figure 7.

Figure S6, related to Figure 8.

Supplementary Experimental Procedures

Construction of bubble stimuli: Bubbles stimuli were constructed as described previously (Gosselin and Schyns, 2001). Briefly, one of 8 face base images (chosen from the Ekman and Friesen stimulus set, 4 different individuals (2 female and 2 male) showing happy and fearful expressions each, all normalized for mean luminance, contrast, and position of eyes and mouth) and their mirror images were sparsely sampled only in the 2-D face plane (no spatial frequency sampling was done) and presented to participants one at a time. The number of bubbles shown was adapted continuously using the QUEST-staircase method with β=3.5, δ=0.01 and γ=0.5 (Watson and Pelli, 1983) targeting an error rate of 20% (the error trials were used to compute the classification image, see below). The mean asymptotic performance actually obtained was 82.6%, confirming the validity of the adaptive procedure. The location of each bubble was chosen randomly and independently of all other bubbles. As subjects improved, the number of bubbles required decreased (learning curve, Fig 3c). The same 8 faces were also used for the

whole face and eye/mouth region trials. Patients performed a short test version of the task (data not shown or analyzed) immediately prior to the experiment with the same stimuli. We implemented the task with the Psychophysics Toolbox in MATLAB (Brainard, 1997).

Electrode localization from structural MRIs: To identify electrode recording sites in the amygdala, T2 relaxation times were measured using spin-echo dual-echo sequences on a 1.5-T Toshiba MR scanner. 25 contiguous axial slices were acquired (0.575 x 0.575 mm in-plane, 5 mm thick, TR=5777.5 ms, TE=105 ms, flip angle = 90°). The imaging slices covered the entire brain, including the amygdala. The electrodes were clearly visible as dark lines in the T2 scans. Images were subsequently processed using SPM8 (Friston, 2007). Scans were first segmented and normalized to the standard MNI space. The electrode tip coordinates were visualized and manually labeled in FSL (Jenkinson et al., 2012). A mask was created in MATLAB for each patient with each recording site as a 3 x 3 x 3 mm cube centering on the identified electrode tip. All masks were then overlaid on the standard MNI152 template with 1 mm isotropic resolution. Each color in Supplementary Figure S1 denotes the bilateral recording sites for an individual patient.

Data analysis: Spike waveforms. Comparisons of the waveform of different neurons were made based on the through-to-peak time of the mean waveform (Mitchell et al., 2007). The mean waveform is the average of all spikes assigned to the cluster (see Fig. 2 for examples). The polarity of the mean waveforms was inverted if necessary such that the through always occurs before the peak. We also verified whether there is a correlation between the through-to-peak time and the mean firing rate of a unit. For this, the mean firing rate was defined as the mean rate over the entire duration of 3.5s of all valid trials.

Data analysis: whole-face selective cells. We selected and quantified whole-face selective cells as described previously (Rutishauser et al., 2011). Briefly, cells were considered as whole-face selective if their firing rate after stimulus onset differed significantly between trials showing whole faces and parts (ROIs). We further quantified the whole-face selectivity of each unit using the whole-face index (WFI). The WFI of unit i is the baseline normalized difference in mean response to whole faces trials compared to bubbles trials (Eq S1).

$$WFI_i = \frac{\overline{R}_{WholeFace} - \overline{R}_{Bubbles}}{\overline{R}_{Baseline}} 100\% \qquad \text{(Eq S1)}$$

If the WFI is different from 0, the unit responds to whole-faces differently than to partially revealed faces. Note that a large nonzero WFI, regardless whether negative or positive, indicates whole-face-selective responses. Thus we used the absolute value of the WFI throughout this paper. Also note that the WFI and the selection of the cells as whole face selective is statistically independent: selection is comparing whole-face trials with parts trial (ROIs) whereas the WFI is based on the difference between whole-face trials and bubbles trials.

Data analysis: Correlation of behavioral and neuronal classification images.

We assessed the correlation between individual NCIs with an average group behavioral classification image. The group behavioral classification image (GBCI) was the average of a total of 9 control subjects that were not used for the neuronal analysis (n=6 nonsurgical control subjects that did not have ASD, also used for eye tracking, and the 3 surgical non-ASD subjects that did not yield any neuronal data) and thus originated from a group of subjects independent of those who contributed the neuronal recordings. For each unit j with a significant NCI, we calculated and appropriately normalized the 2D correlation between the NCI and the GBCI (Eq S2).

$$CIcorr_j(x,y) = NCI(x,y) * GBCI(x,y) \qquad \text{(Eq S2)}$$

Both the NCI and the GBCI are in terms of z-scores. The distribution of the product of two z-scores, however, is not well defined and we thus estimated this distribution empirically using a bootstrap procedure (as described above). This procedure yielded an estimate of the mean μ_j and variance σ_j of CIcorr at every pixel (x,y). The z-scored 2D correlation (as shown in Fig. 6a,b) is

$$Z\_CIcorr_j(x,y) = \frac{CIcorr_j(x,y) - \mu_j(x,y)}{\sigma_j(x,y)} \qquad \text{(Eq S3)}$$

Data analysis: interspike intervals analysis. We computed the interspike interval distribution (ISI) of each cell by considering all spikes fired during the experiment and

quantified it using two metrics: the modified coefficient-of-variation C_{V2} and the burst index (BI). The BI was defined as the proportion of ISIs less than 10ms (Wyler et al., 1975). The CV2 (Eq S4) is a function of the difference between two adjacent ISIs and is a standard measure to quantify spike-train variability that is robust to underlying rate changes (Holt et al., 1996). In contrast, the coefficient-of-variation measure CV is only valid for stationary processes, i.e. fixed mean rate and is thus not applicable for this analysis.

$$CV2 = \frac{1}{N}\sum_{i=1}^{N}\frac{2|ISI_{i+1}-ISI_i|}{ISI_{i+1}+ISI_i} \qquad \text{(Eq S4)}$$

Data analysis: variability of responses. We quantified the variability of the spiking response that followed the onset of the face on the screen using the coefficient of variation (standard deviation divided by mean) of the number of spikes counted in the same window (1.5s) as used to quantify the NCIs. For each cell, we computed the CV of its response for either all trials, only WF trials, or only bubble trials and then compared the CV values of different groups of neurons. CV values were approximately 1 as expected and there were no significant differences between the CV values of neurons from ASD and controls for all cells, only cells with NCIs, or only WF cells either for all trials, only bubble trials or only WF trials.

Data analysis: Exclusion of epileptic areas. To check that results were not influenced by abnormal responses within regions of seizure focus (Rutishauser, 2008), we repeated analyses by conservatively excluding all units originating from the brain hemisphere in which the temporal epileptic seizure focus was detected (if there was one; see Table S1). 121 units remained, 76 of which had mean firing rates>0.5Hz. 21 of these (28%) of these had significant NCIs (12 of which in the two patients with ASD), which is a very similar proportion compared to when using all cells (29%). Only 5 NCIs were dropped. All results remained quantitatively similar when excluding these NCIs from the analysis. Also note that with one exception, no patient had a seizure origin in the amygdala.

Statistical verification with bootstrap methods.

We also used a non-parametric bootstrap procedure to estimate the significance of the NCIs and arrived at very similar results compared to the cluster test. The procedure (see below) is more conservative and thus results in fewer cells with significant NCIs (15 instead of the

previous 26), but importantly all differences that we report between ASD and controls remain significant and qualitatively similar (average Z-value in mouth and eye ROIs is significantly larger and smaller in ASD compared to controls, respectively, at P=0.003 and P=0.004). The bootstrap procedure was run 200 times for every cell. At each iteration, the order of the noise masks was scrambled randomly such that the association between which noise mask resulted in which spike count was randomized. Thus, the distribution of spike counts observed as well as the distribution of noise masks used was preserved, but their relation was randomized. This yields a reliable estimate of the NCIs to be expected by chance for each cell, taking into account in particular possible effects of unusual noise masks (that arise by chance) or outlier spike responses such as bursts. We then used these random NCIs to estimate the distribution of values at each pixel (x,y) expected by chance and compared it with the value actually observed. The bootstrap test for the significance of NCIs is based on an empirical estimate of the Euler characteristic (EC). The EC quantifies the number of clusters in a thresholded Gaussian random field (Adler, 1981; Worsley, 1994). For example, a EC=2 for a given threshold means that 2 clusters are present for this threshold. The cluster test (see above) is a parametric implementation of this concept (Chauvin et al., 2005; Friston et al., 1993). We also calculated the empirical estimate of the EC (using bootstrap) to further verify our results as follows. For every bootstrapped NCI, we estimated the associated EC for different thresholds T. Then, T was set such that only 5% of randomly permuted trials had an EC>=1. Thus, this procedure assures that the threshold T is fully corrected for multiple comparisons. This empirically estimated threshold T was then used to determine whether an NCI was significant or not.

Data analysis: Comparison between cutout and NCI responses.

We categorized an NCI, regardless of its significance, according to whether it showed a differential response to the mouth, left eye, right eye or neither of those. First, the mean Z-scored NCI within each of the 3 ROIs was calculated and a cell was assigned to one of the groups if the mean Z value within one of the ROIs was >0 whereas it was <0 for the others. 23 of the cells had a mouth NCI, 19 an eye NCI and 49 had neither. For each of the three groups, the average response difference to eye and mouth cutouts was then calculated. For mouth-and eye sensitive cells this quantity was expected to be significantly negative and positive, respectively.

Eye tracking – subjects. We repeated the identical task after patients were released from the hospital at our laboratory at Caltech while tracking eye movements. There were four groups of subjects that performed the task: 1) a control group of non-surgical autism subjects that did not have epilepsy (six subjects, 5 male, mean age 32±12, see Table S2 for autism scores), 2) a control group of matched neurotypical normals (six subjects, 5 male, mean age 25±2), 3) epilepsy subjects without autism from which we also previously recorded neural activity (three subjects, P19,P20 and P21 in Table S1), and 4) the two epilepsy subjects that also had autism. All epilepsy subjects had been operated (partial resection) by the time eye tracking was performed, with the exception of one of the autism subjects with epilepsy (P17). All 17 subjects performed the task under conditions identical to the patients, with the same instructions. Subjects completed between 360-840 trials each (mean 456±176 trials, ±s.d. over subjects). Task performance accuracy as well as the speed of learning during eye tracking were comparable between the non-surgical autism group and the matched neurotypical control group. There was no significant difference in the number of bubbles reached in the last trial (31.6±25.2 and 17.5±10.3, for controls and ASD, respectively; P=0.28, ±s.d.) as well as the reaction time in bubble trials (866±142ms and 815±179ms; P=0.6, ±s.d.) or all trials (847±122ms and 790±151ms; P=0.49, ±s.d.). This independently confirms our observation on the neurosurgical subjects that showed no difference in performance and reaction time between ASD and control subjects.

Eye tracking was carried out using a non-invasive infrared remote Tobii X300 system together with Tobii Studio 2.2 software. Eye movements were recorded bilaterally with 300 Hz. Stimuli were shown on a 23-inch screen (screen resolution: 1920x1080).

Eye tracking – fixation density analysis. Fixations were detected by a fixation filter in Tobii Studio 2.2 that detects quick changes in the gaze location using a sliding window averaging method (Olsson, 2007). Only correct trials were considered for all fixation density calculations. Fixation locations were smoothed with a 40-pixel 2D Gaussian kernel with a standard deviation of 10 pixels (the same as is used for display of the stimuli and in the analysis throughout). Each heat map indicates the probability of fixating a given location (in arbitrary units), which is

calculated based on the number and duration of fixations and which ensured an equal contribution from each subject and statistical independence between subjects.

To correct for possible drift in the calibration of the eye tracker, we performed a post-hoc drift-correction procedure for each trial. Before the presentation of faces, a fixation circle superimposed on a scrambled face image was presented for a random duration between 800 to 1200 ms. We subtracted the mean fixation position of the last 500 ms during this fixation period from all subsequent fixations during the face presentation period.

To quantitatively compare the fixation densities within certain parts of the face, we defined three ROIs: eyes (left and right), mouth and center. Each ROI is a circle with a radius of 35 pixels. The average fixation density within the ROIs was calculated for each subject and category (bubbles, whole faces, parts) during either the entire 500ms post stimulus-onset period or only the last 200ms period before offset of the face. Statistical comparisons were then performed to compare whether the mean fixation density values within the ROIs different between groups (normals, autism subjects without epilepsy, epilepsy patients without autism, epilepsy patients that had autism; thus there were 4 categories in the subject group variable of the one-way ANOVA).

When counting the number of different fixations subjects made in a particular trial, we started counting at 1. Thus, if subjects made no fixations and stayed at the center, this trial was counted as having 1 fixation.

Eye tracking – conditional probability analysis. For each participant, we computed the conditional probability that, over all correct trials, the participant directed his/her gaze to the revealed parts within the first 500 ms after stimulus onset. In every given trial, each pixel (x,y) was assigned one of three values: 1 if the pixel was revealed and fixated (within 8 pixels, approximately 0.3°), 0 if the pixel was revealed and not fixated, and undefined if the pixel was not revealed. The average conditional probability maps for each patient were calculated by averaging, for each pixel, all the trials where the pixel was revealed. After obtaining such probability maps for each participant, we averaged over participant groups (ASD group and control group).

We computed the average latency of the first fixation to fall into the eye or mouth ROIs (see Figure 5B). For each trial, if there were any fixations falling into an ROI, we took the time that the first fixation entered the ROI as the latency; otherwise, we excluded that trial to compute the average latency. We defined the fastest latency as 3.33 ms (the first sample data point at 300 Hz sampling rate of the eye tracker) if the first fixation of the trial was in an ROI at the beginning of a trial.

Data analysis – selection of bubble trials. We selected trials according to the overlap of the bubbles with the specified eye and mouth ROIs (as shown in Figure 5B). The more overlap between bubbles and ROIs, the more is revealed within the ROI. We chose two categories of ROI trials: those where predominantly only the eye or the mouth was shown. Eye-dominant and mouth-dominant were achieved by enforcing 'High Eye AND Low Mouth' overlap and 'Low Eye AND High Mouth' overlap, respectively. 'High' or 'Low' here was above or below the median of the overlapping values across all trials. Selection of trials based on ROIs revealed was only based on the stimulus shown to the subjects and did not involve the neuronal response or eye movements.

Supplementary Tables

Table S1: Neurosurgical patients: demographics, pathology and neuropsychological evaluation. Abbreviations: Hand: Dominant handedness; Lang Dom: language dominance as determined by Sodium Amybarbital (Wada) test; Benton: Benton Facial Recognition Test, long form score (a measure of ability to discriminate faces visually). Benton scores of 41-54 are in the normal range; WAIS-III: IQ scores from the Wechsler Adult Intelligence Scale: performance IQ (PIQ), verbal IQ (VIQ), full scale IQ (FSIQ), verbal comprehension index (VCI), perceptual organization index (POI). All WAIS-III scores are on average 100 with a s.d. of 15 in the normal population (69 and less falls in the clinically abnormal range, 70-79 borderline, 80-89 low average, 90-109 average, 110-119 high average, 120-129 superior, 130+ very superior). Scores from the Rey-Osterrieth Complex Figures test are raw scores from the subtests copy (visuospatial perception and construction), immediate recall reproduction (IR, additional short-term visual memory demands), and 30-minute delayed recall reproduction (DR, additional longer-term visual memory demands). 36 possible points for each, 18+ is normal depending on age. (*) Are the two neurosurgical autism patients who contributed the single-unit data (see Table S2), (+) are neurosurgical patients without autism who contributed neurons, but had no significant neuronal classification images from our task (NCIs), (++) are neurosurgical patients without autism who contributed neurons that also had significant NCIs and (-) are neurosurgical patients without autism who contributed only behavior (no neurons recorded). Tests indicated with n/a were not performed for clinical reasons.

ID	Age	Sex	Hand	Lang Dom	Epilepsy diagnosis	Benton	WAIS-III					Rey-Osterrieth		
							PIQ	VIQ	FSIQ	VCI	POI	copy	IR	DR
P17 (*)	19	M	R	L	Left inferior frontal	43	128	131	134	122	133	34	23	21
P18 (++)	40	M	R	L	Right mesial temporal hippocampus	52	69	n/a	n/a	n/a	n/a	n/a	n/a	n/a

P19 (++)	34	M	R	n/a	Left supplementary motor neocortex	39	81	74	86	76	80	31	23	20.5
P20 (-)	27	M	R	L	Right mesial temporal hippocampus	49	88	98	81	89	101	33	21	23.5
P21 (-)	20	M	R	n/a	Right dorsolateral neocortex	45	n/a	n/a	n/a	93	89	34	27.5	27
P23 (++)	35	M	R	L	Left mesial temporal amygdala	41	n/a	n/a	n/a	74	86	34	n/a	9.5
P25 (+)	31	M	R	L	Right dorsolateral neocortex	47	81	91	87	98	82	36	9	5
P27 (-)	41	M	R	n/a	Bilateral independent temporal lobe	49	86	91	89	86	88	36	5	5
P28 (*)	23	M	R	L	Right mesial temporal hippocampus	47	79	77	76	78	80	34	9.5	13
P29 (++)	18	F	L	L	Left deep insula	49	104	110	107	107	101	36	19.5	19.5

Table S2: Autism diagnosis for the two neurosurgical patients with ASD (*), and six other (non-neurosurgical) ASD comparison subjects (Aut; not all scores were available for all patients, numbers are stated as mean±s.d. over the number of subjects as indicated in brackets). Both neurosurgical patients met clinical (DSM-IV-TR) and ADOS-criteria for a diagnosis (ASD for P17; Autism for P28). Entries marked with "-" are not available. Abbreviations: Autism Diagnostic Observation Schedule (ADOS), Autism Diagnostic Interview (ADI), Social Responsiveness Scale (SRS), Autism Quotient (AQ).

ID	ADOS Scores				ADI Scores				SRS	ADOS Diagnosis	AQ
	A	B	C	D	A	B	C	D	A-SR		
P17*	3	5	8	2	12	8	4	3	50	ASD	31
P28*	6	6	0	0	-	-	-	-	89	Autism	22
Aut	3±1 (6)	8±3 (6)	1±0 (6)	1±1 (6)	21±10 (2)	17±7 (2)	7±2 (2)	2±2 (2)	108±16 (4)	Autism	24±15 (3)

Table S3: Number of neurons recorded and analyzed. Left/Right refers to the left and right amygdala, respectively. All is both left and right amygdala.

	# units total			**# units> 0.5 Hz**			**# significant NCIs**		
	Left	Right	All	Left	Right	All	Left	Right	All
ASD	43	13	56	29	8	37	11	5	16
Controls	20	68	88	10	44	54	3	7	10
Total	63	81	144	39	52	91	14	12	26

Table S4: Responses to bubbles. All tests are P<0.05 and independent of one another; that is, a neuron can contribute to more than one of the listed categories. Percentages are out of a total of 91 units. The first two rows are based on all trials, whereas the last three rows are based exclusively on the bubbles trials.

Response Characteristics		**# units**			**% units**
		ASD	Ctrl	All	
Visually responsive (scramble vs. baseline blank screen)		3	10	13	14%
Face responsive (stimulus vs. scramble)		15	27	42	46%
Fear vs. happy (bubbles trials)		3	9	12	13.2%
Identity (1-way ANOVA, 4 identities, bubbles trials)		0	7	7	7.7%
Gender X Fear/Happy (2x2 ANOVA, bubbles trials)	gender ,	1	3	4	4.4%
	fear versus happy	2	10	12	13.2%
	interaction	2	4	6	6.5%

Table S5: Electrophysiological properties of neurons. Numbers shown are calculated based on all spikes during the entire experiment (baseline and stimulus periods). However, quantitatively similar results (with no significant differences) hold when only considering baseline or after-stimulus onset periods (1.5 before or after stim onset). Abbreviations: CV_2 modified coefficient of variation, BI burst index, d peak-to-through distance of waveforms. d values are distributed significantly bimodally, as verified by Hartigan's dip test. Pairwise comparisons between ASD and Ctrl for the three cell groups (all, WF, and NCI, see text for details) are all n.s. with P>0.05 (two-tailed t-test for rate, CV2, and BI; and two-tailed Kolmogorov-Smirnov test for d; ± is s.d. over all units as indicated).

	n	**CV2**	**BI**	**d [ms]**
ASD, all	37	0.98±0.06	0.02±0.02	0.65±0.33
Ctrl, all	54	0.97±0.09	0.02±0.02	0.65±0.37
ASD, WF	12	0.93±0.08	0.02±0.02	0.83±0.31
Ctrl, WF	17	0.97±0.06	0.01±0.01	0.63±0.35
ASD, NCI	16	1.00±0.04	0.03±0.02	0.63±0.35
Ctrl, NCI	10	1.05±0.12	0.03±0.02	0.62±0.34

Table S6: Eye movement quantification, as shown in Fig S6. Shown is the average fixation density across subjects, averaged within the ROIs for trials where parts were shown. Abbreviations: Epi = Epilepsy, Ctrl=Control. One-way ANOVAs with factor subject group (ASD, ASD+Epi, Epi, Control) for each ROI were not significant with P>0.05. Paired post-hoc t-tests between ASD and Controls for each ROI and trial type were similarly not significant at P>0.05 (For Parts all 500ms, P=0.61, P=0.12, P=0.97; Parts 200ms only, P=0.88, P=0.09, P=0.94; for central, mouth, eye ROI, respectively; ± shows s.e.m. over subjects, with n as indicated).

	Density central ROI [%]				**Density mouth ROI [%]**				**Density eye ROI [%]**			
Trial Type (n)	**ASD (6)**	**ASD +Epi (2)**	**Epi (3)**	**Ctrl (6)**	**ASD (6)**	**ASD +Epi (2)**	**Epi (3)**	**Ctrl (6)**	**ASD (6)**	**ASD+ Epi (2)**	**Epi (3)**	**Ctrl (6)**
Parts (all 500ms)	44±4	40±7	47±3	47±3	12±2	12±5	8±4	17±2	21±3	20±6	23±4	21±4
Parts (last 200ms)	11±5	11±9	18±3	12±4	22±4	19±8	14±7	30±2	34±5	31±7	36±7	33±6

Table S7: Electrode localization in MNI space (X,Y,Z). See Fig 1 and Supplementary Figure 1 for illustration. LA: left amygdala; RA: right amygdala.

Patient	**NMI coordinates LA**	**NMI coordinates RA**
P17	-22, -2, -24	18, 0, -22
P18	-16, -8, -17	24, -4, -20
P19	-18, -2, -24	21, 2, -22
P20	-18, -10, -16	18, -4, -22
P21	-20, 0, -20	16, -2, -18
P23	-16, 4, -24	16, -4, -22
P25	-21, -5, -25	18, -5, -24
P27	-15, -2, -22	18, -2, -22
P28	-18, -4, -24	20, -4, -24
P29	-18, -6, -18	20, -2, -22

Table S8: Eye movement quantification for the last 200ms before stimulus offset. Shown is the fixation density, conditional on a particular region of the face having been shown. The densities given here are different from those in Table S6, where the fixation density is shown pooled over all trials regardless of which region of the face was shown. P-values are pairwise comparisons between the groups with ASD and their respective controls (Epilepsy-only for neurosurgical patients, normal controls for ASD-only subjects; ± shows s.e.m. over subjects).

	Density left eye ROI [%]				**Density right eye ROI [%]**				**Density mouth ROI [%]**			
Trial Type	**ASD**	**ASD +Epi**	**Epi**	**Ctrl**	**ASD**	**ASD +Epi**	**Epi**	**Ctrl**	**ASD**	**ASD+ Epi**	**Epi**	**Ctrl**
Parts	47±7	44±9	47±4	54±7	50±7	50±9	58±16	50±10	69±12	56±25	43±20	85±5
P value	0.51	0.88			0.97	0.99			0.25	0.64		

Table S9: Behavioral reaction times (RT) for different trial types (eye cutout, mouth cutout, all bubbles). Shown are the average RT (latency to push button from stimulus onset) for all trials of each kind, regardless of whether the response was correct. Means and ±s.e.m. across subjects are given, with n as indicated in brackets in the header row. P-values in the table are pairwise comparisons between the ASD and controls for the ROI shown on the same row. A 2-way ANOVA with factors subject group (ASD, controls) and ROI (eye, mouth) showed no significant main effects nor interactions for all three groups considered (epilepsy during eyetracking, epilepsy during electrophysiology, non-surgical controls), all P>0.2.

	Epilepsy (surgical) group; RT during eye tracking [ms]			Epilepsy (surgical) group; RT during electrophysiology [ms]			Non-Epileptic (non-surgical) group; RT during eye tracking [ms]		
	ASD (2)	**Ctrl (3)**	**p**	**ASD (2)**	**Ctrl (8)**	**p**	**ASD (6)**	**Ctrl (6)**	**p**
Eye cutout	1124±2.4	912±271	0.37	1144±128	976±55	0.22	834±26	775±58	0.45
Mouth cutout	912±41	878±189	0.82	1014±42	991±47	0.82	879±54	790±59	0.29
Bubbles all	974±19	926±132	0.8	1357±346	1032±49	0.28	866±58	815±73	0.60

Table S10: Behavioral reaction times (RT) for different kinds of bubble trials. Shown are the average RT for all trials of each kind, regardless of whether the response was correct, relative to stimulus onset. Means and ±s.e.m. across subjects are given, with n as indicated in brackets in the header row. P-values in the table are pairwise comparisons between the ASD and controls for the ROI shown on the same row. A 2-way ANOVA with factors of subject group (ASD, controls) and ROI (eye, mouth) showed no significant main effects nor interactions for both the surgical and non-surgical group (all P>0.4).

	Epilepsy (surgical) group; RT during eye tracking [ms]			Non-Epileptic (non-surgical) group; RT during eye tracking [ms]		
	ASD (2)	**Ctrl (3)**	**p**	**ASD (6)**	**Ctrl (6)**	**p**
Bubbles – eye only	990±11	923±240	0.74	867±145	816±182	0.60
Bubbles – mouth only	978±20	942±243	0.86	864±146	808±170	0.55
Bubbles – eye and mouth	948±9	900±40	0.81	872±59	789±68	0.38

Supplementary Figure Legends

Figure S1: Individual recording sites in the patients. Sagittal and coronal slices of the MNI152 template MRI scan are shown with electrode positions indicated. The top left shows the position of the coronal slices shown in the other panels. Shown are y=-10, -8, -6, y=-4, y=-2, y=0, and y=2 from left to right. Subjects are marked by colors (compare to Supplementary Table 1 and 7).

Figure S2: Supplemental behavioral results. (A) Nr of bubbles revealed on the last trial, shown on the same scale as in Fig 3C. (B) Average reaction time for each subject for all bubble trials. (A,B) Errorbars are s.e.m. over the datapoints shown. (C,D) Overlay of thresholded (Z>3.5) behavioral classification images on an example face image for the ASD group (a) and controls (b); this figure depicts the same data as does Figure 2d,e.

Figure S3: Single-unit examples. Shown are examples of neurons with significant NCIs from one of the patients with ASD (A) and three controls (B-D). Shown, from top to bottom, are: i) Raster of grouped trials. Bubbles trials are sorted according to overlap of the noise mask with the significant part of the NCI. The overlap is indicated by the magenta line (zero overlap at top, maximal overlap at bottom). Trials are dually aligned to scramble onset (shown for variable amount of time 0.8-1.s) as well as face onset (shown for 500ms). Insets in red show waveforms of the isolated neuron (actual traces in red, clustering waveform in black). ii) peri-stimulus time histogram (PSTH) for the different stimulus categories, iii) PSTH of bubbles trials only, divided into those that overlap with the ROI defined by the NCI and those that do not (inside and outside, respectively). iv) Raw Z-scored NCI (left) and the statistically thresholded NCI superimposed on face (right).

Figure S4: Average 2D Correlation between the independent group BCI from nonsurgical controls and the NCIs of each patient. The correlation was calculated separately for each cell with a significant NCI and then averaged for each patient. (A-F) Correlations for the two

patients with ASD (A,B) and the five controls (C-F). Color code is Z-scores, as determined by bootstrap (see methods). Patient IDs and number of NCIs used for each are as indicated.

Figure S5: Responses to bubbles compared with responses to face cutouts. Results are shown for cells recorded in all 7 patients. Comparison of bubbles response with response to eye/mouth cutouts for all neurons we analyzed (n=91). Cells with NCIs that had more response inside the mouth ROI responded more to the mouth cutouts, resulting in a negative difference between eye and mouth cutouts (n=23, $P<0.05$). Cells with NCIs that responded to one of the eyes responded more to eye cutouts (n=19, $P<0.05$). Cells that did not have an NCI in one of the ROIs had no significant difference (n=49) (although the mean response difference was negative, indicating a higher response for mouth than eye cutouts). * indicates $P<0.05$ when compared to zero.

Figure S6: Eye movements quantified using fixation density maps. Participants saw the same stimuli and performed the same task as during our neuronal recordings while we carried out eye tracking. Data were quantified using fixation density maps that show the probability of fixating different locations. In addition to the entire 500ms period after stimulus onset for bubbles trials (Figure 8, main paper) we also computed the same metric for other trial types and time periods: (A) 500ms period after face onset for eye/mouth parts trials only, (B) 200ms before face offset for bubbles trials, (C) 200ms before face offset for eye/mouth parts only. (D) Shows fixation locations quantified as the conditional probability that a location was fixated, given that it was revealed (shown). This metric (see methods) can only be computed for the bubbles trials. (E-F) Fixation density maps for subsets of cutout trials: left eye (E), right eye (F) and mouth (G) parts only. Density was calculated using the last 200ms before stimulus offset. Subjects only made fixations to the stimuli shown. (A-G) For each row, four separate groups of subjects are shown (from left to right): autism control subjects (n=6), autism subjects with epilepsy (n=2), subjects with only epilepsy (n=3) and neurotypical normal control subjects (n=6).

Supplementary References

Adler, R.J. (1981). The geometry of random fields (New York: Wiley).

Brainard, D.H. (1997). The Psychophysics Toolbox. Spatial Vision 10, 433-436.

Chauvin, A., Worsley, K.J., Schyns, P.G., Arguin, M., and Gosselin, F. (2005). Accurate statistical tests for smooth classification images. J Vision 5, 659-667.

Friston, K.J. (2007). Statistical parametric mapping : the analysis of funtional brain images, 1st edn (Amsterdam ; Boston: Elsevier/Academic Press).

Friston, K.J., Worsley, K.J., Frackowiak, R.S.J., Mazziotta, J.C., and Evans, A.C. (1993). Assessing the significance of focal activations using their spatial extent. Hum Brain Mapp 1, 210-220.

Gosselin, F., and Schyns, P.G. (2001). Bubbles: a technique to reveal the use of information in recognition tasks. Vision Research 41, 2261-2271.

Holt, G.R., Softky, W.R., Koch, C., and Douglas, R.J. (1996). Comparison of discharge variability in vitro and in vivo in cat visual cortex neurons. Journal of neurophysiology 75, 1806-1814.

Jenkinson, M., Beckmann, C.F., Behrens, T.E., Woolrich, M.W., and Smith, S.M. (2012). FSL. Neuroimage 62, 782-790.

Mitchell, J.F., Sundberg, K.A., and Reynolds, J.H. (2007). Differential attention-dependent response modulation across cell classes in macaque visual area V4. Neuron 55, 131-141.

Olsson, P. (2007). Real-time and offline filters for eye tracking. (KTH Royal Institute of Technology).

Rutishauser, U. (2008). Learning and representation of declarative memories by single neurons in the human brain. In Computation&Neural Systems (PhD Thesis) (Pasadena, California Institute of Technology).

Rutishauser, U., Tudusciuc, O., Neumann, D., Mamelak, A.N., Heller, A.C., Ross, I.B., Philpott, L., Sutherling, W.W., and Adolphs, R. (2011). Single-unit responses selective for whole faces in the human amygdala. Curr Biol 21, 1654-1660.

Watson, A.B., and Pelli, D.G. (1983). Quest - a Bayesian Adaptive Psychometric Method. Percept Psychophys 33, 113-120.

Worsley, K.J. (1994). Local Maxima and the Expected Euler Characteristic of Excursion Sets of Chi(2), F and T Fields. Adv Appl Probab 26, 13-42.

Wyler, A.R., Fetz, E.E., and Ward, A.A., Jr. (1975). Firing patterns of epileptic and normal neurons in the chronic alumina focus in undrugged monkeys during different behavioral states. Brain Res 98, 1-20.

SUPPLEMENTAL FIGURE 1

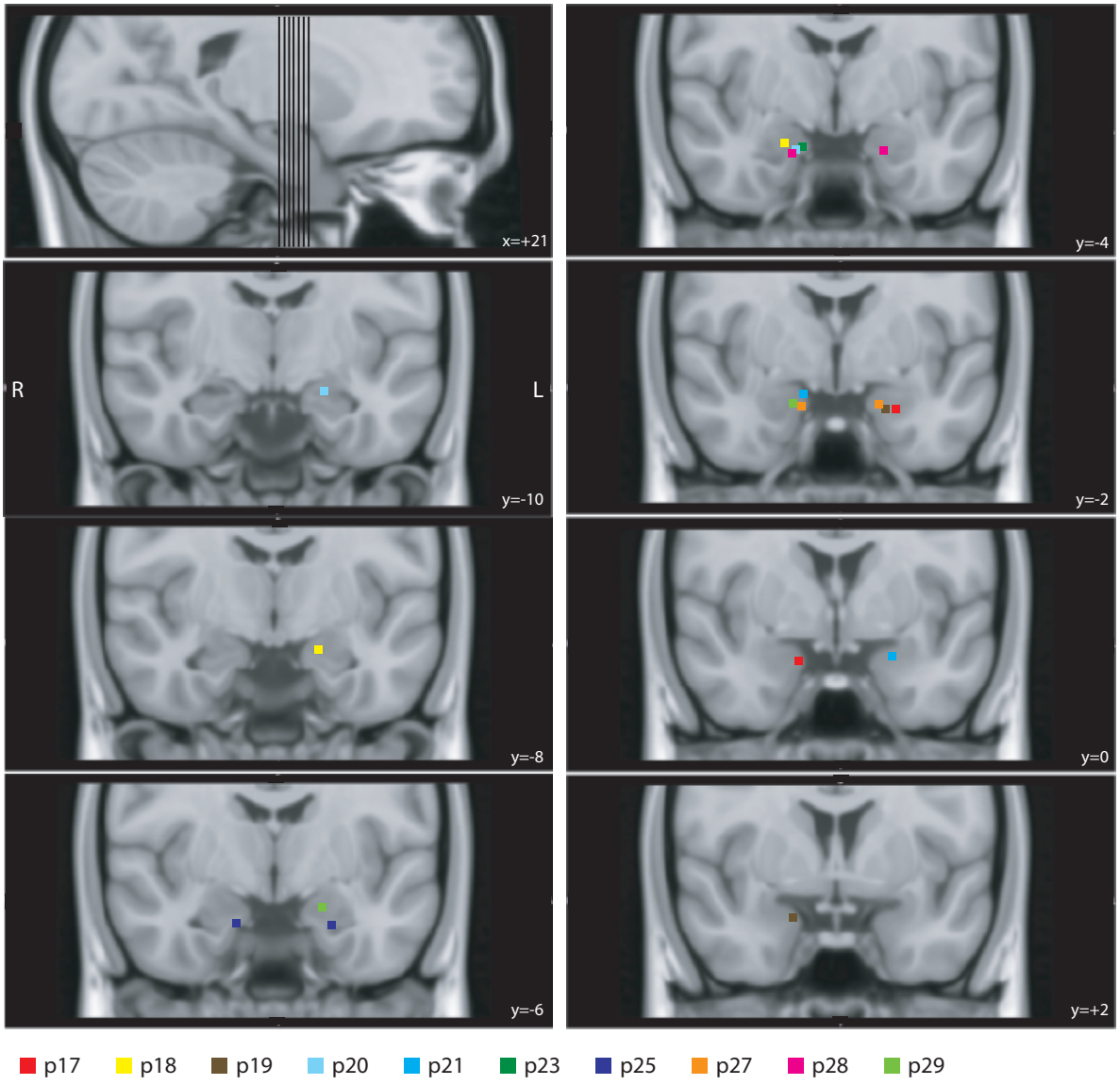

SUPPLEMENTAL FIGURE 2

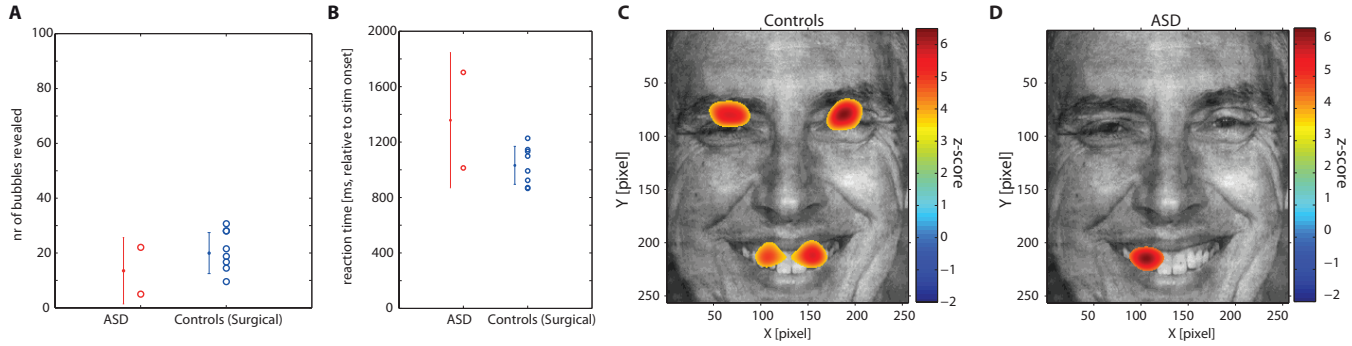

SUPPLEMENTAL FIGURE 3

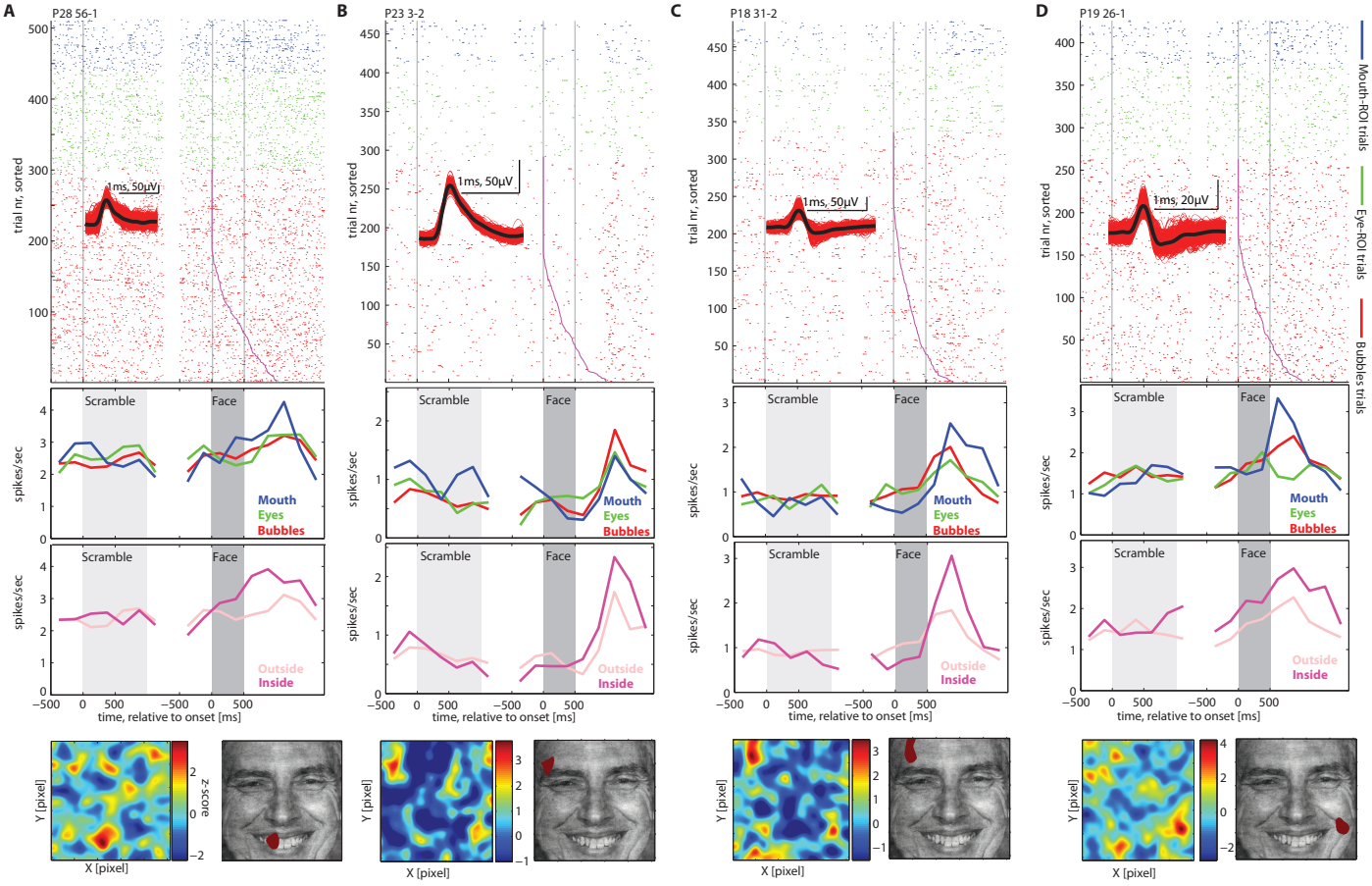

SUPPLEMENTAL FIGURE 4

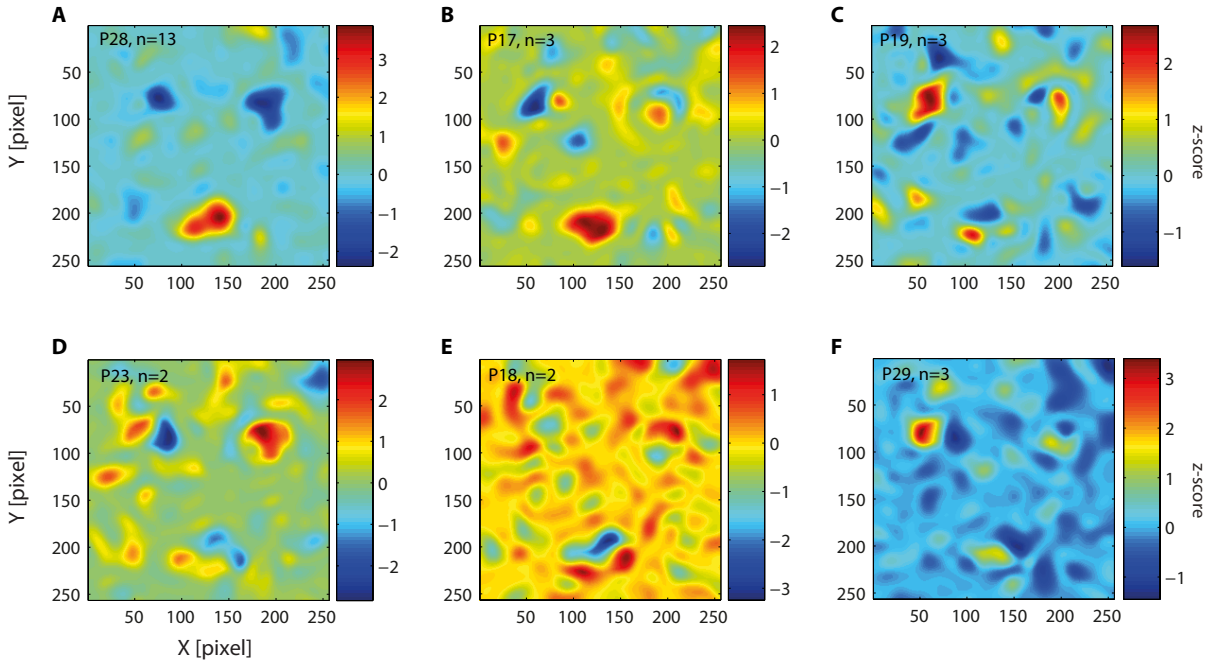

SUPPLEMENTAL FIGURE 5

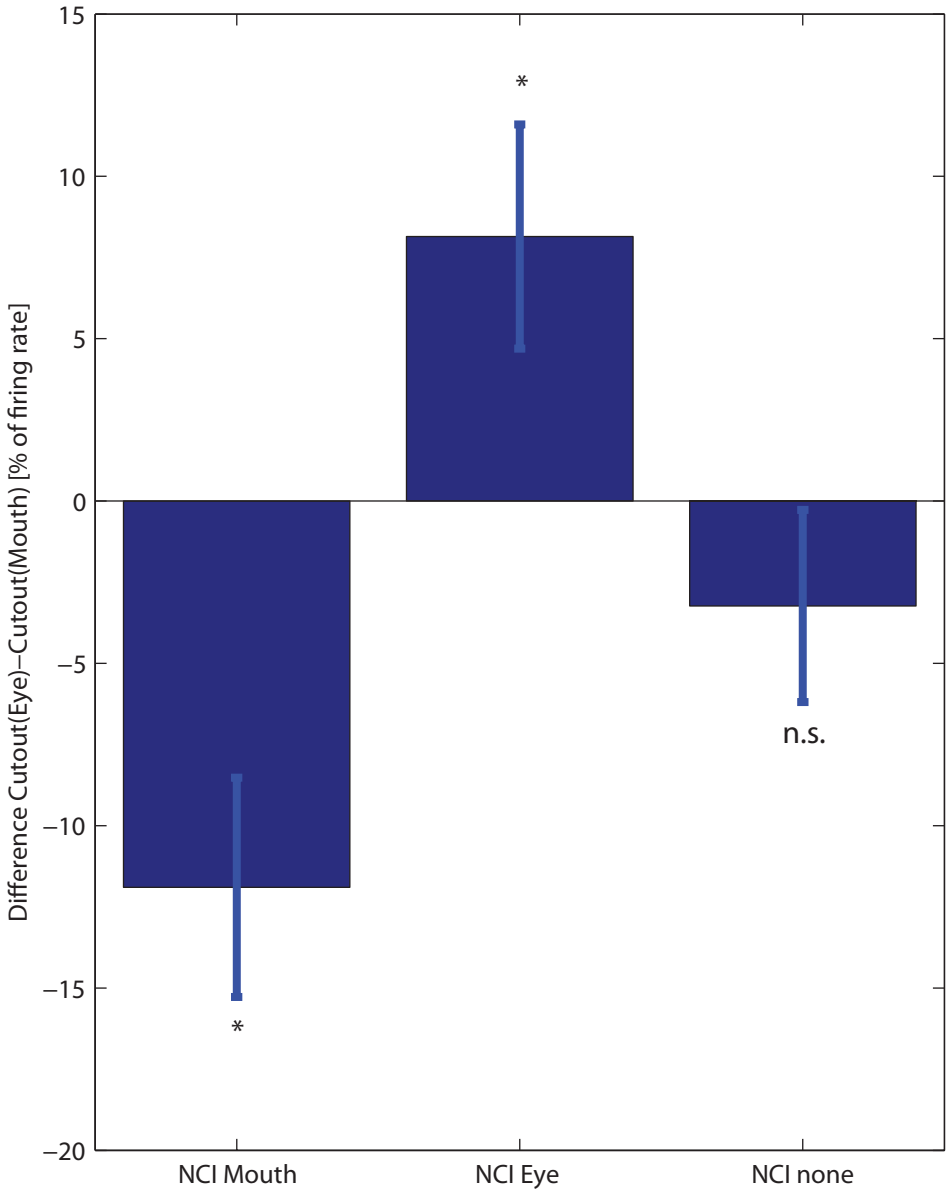

SUPPLEMENTAL FIGURE 6